64-10

431784

NOLTR 63-144

THE DESIGN AND DEVELOPMENT OF THE ARCHER SOUNDING ROCKET

14 JUNE 1963

NOL

UNITED STATES NAVAL ORDNANCE LABORATORY, WHITE OAK, MARYLAND

NOLTR 63-144

Aerodynamics Research Report 200

THE DESIGN AND DEVELOPMENT OF THE ARCHER SOUNDING ROCKET

Prepared by:
H. J. Gauzza
R. H. Cornett
R. T. Groves

ABSTRACT: The Naval Ordnance Laboratory has designed, developed and conducted free-flight tests on the Archer sounding rocket. Archer is an economical, single-stage sounding rocket capable of carrying a 25-pound payload to an altitude of 100 miles for IQSY studies.

The aerodynamic as well as mechanical design considerations used in the production of this rocket are described. Included in the aerodynamic phase are the configuration design, the investigation of stability and the determination of aerodynamic loads and heating. Structural integrity with minimum weight and ease of manufacture are prime considerations in the mechanical design.

Archer's performance is predicted and comparisons are made with the results of the first two test firings.

U. S. NAVAL ORDNANCE LABORATORY
WHITE OAK, MARYLAND

NOLTR 63-144

14 June 1963

THE DESIGN AND DEVELOPMENT OF THE ARCHER SOUNDING ROCKET

This design and development project was performed at the request (reference (1)) of the Naval Research Laboratory under Task Number NOL 625.

The purpose of this project was to provide a sounding rocket with good aerodynamic characteristics suitable for shipboard launchings, and capable of carrying a 25-pound payload to an altitude of 100 miles.

The authors wish to acknowledge the suggestions and technical assistance rendered by the Atlantic Research Corporation in the production of this rocket.

R. E. ODENING
Captain, USN
Commander

K. R. ENKENHUS
By direction

CONTENTS

TABLES

ILLUSTRATIONS

INTRODUCTION

In 1961 the Naval Research Laboratory (NRL) requested that the Naval Ordnance Laboratory (NOL) design and develop a sounding rocket, named Archer, to be used for experimentation during the International Quiet Sun Year (IQSY). Specifically, this task comprised the work necessary to complete three prototype rockets using three engines and boosters built by the Atlantic Research Corporation (ARC), Alexandria, Virginia. These three engines were given by the National Aeronautics and Space Administration (NASA) to the NRL for their use in developing a new intermediate-range sounding rocket. These engines were left over from a program funded by NASA. The objective of this program was to have the ARC incorporate state-of-the-art improvements in their ARCON Sounding Rocket Engine. The main improvements to the engine include: a high performance grain; a new, superior grain retention system; a new, superior insulation liner; and an advanced nozzle design.

Performance calculations made by the NOL indicated that Archer would achieve an altitude in excess of 100 miles with a 25-pound payload on a vertical trajectory. This potential performance with a single-stage, easily handled rocket would make the vehicle extremely useful as a medium capability sounding rocket. In order to conduct sounding experiments in this altitude range at present, multiple-stage units or highly expensive, ballasted single-stage vehicles, with a higher payload capability, must be used. Archer, potentially, answers the need for a highly reliable, low-cost system to accomplish medium altitude sounding missions in the F-2 region.

The technique employed in the design and development of the Archer sounding rocket follows generally the method by which the Iris sounding rocket was designed and developed (reference (2)). Both rockets share the distinction of having been designed and developed in record time due to the urgency of scheduling. This, of course, limits the time spent in the studies necessary to produce a superior rocket. Nevertheless, it was felt that the approach used in designing the Iris sounding rocket was sound as evidenced by the unprecedented success of the Iris vehicle launchings and should certainly be taken advantage of in the present program.

SYMBOLS

A area

A_b body cross-sectional area

A_f	planform area of two fins
a	speed of sound
b	fin span
C_D	vehicle drag coefficient, D/qA_b
C_L	lift coefficient, L/qA_b
C_{L_α}	slope of lift curve, $\partial C_L/\partial\alpha$
C_M	pitching moment coefficient, M/qA_bd
C_{M_q}	pitch-damping-moment coefficient, $\partial C_M/\partial(qd/2V)$
C_{M_α}	slope of pitching-moment curve, $\partial C_M/\partial\alpha$
C_N	normal force coefficient, N/qA_b
C_{N_α}	slope of normal-force curve, $\partial C_N/\partial\alpha$
C_p	specific heat at constant pressure
c	distance from section neutral axis to extreme fiber
C_{l_α}	slope of lift coefficient per unit area of fin
D	drag force
d	body diameter
d_i	nose cone I.D. at base
d_i'	nose cone I.D. at tip attachment point
d_o	uncoated nose cone O.D. at base
d_o'	uncoated nose cone O.D. at tip attachment point
e	distance from fin centerline to fin mounting bolts
F_{SL}	thrust at sea level
f	magnification factor
$f\bar{\alpha}$	total angle of attack ($\Delta\omega \neq 0$), $\sqrt{\alpha^2+\beta^2}$
H	skin span of fin
h	altitude

I	vehicle transverse moment of inertia about center of gravity area moment of inertia
I_f	area moment of inertia of fin about rocket axis
I_x	vehicle axial moment of inertia
k	thermal conductivity radius of gyration
L	lift force
L_r	fin root length
L_t	fin tip length
ℓ	skin length at fin root nose-cone length of fiberglas
M	Mach number moment
m	mass
N	normal force
P	load
P_c	rocket chamber pressure
p	pressure
p_o	atmospheric pressure at sea level
Q.E.	quadrant elevation
q	dynamic pressure
$^\circ R$	degrees Rankine
Re	Reynolds number
s	stress
T	temperature
t	time thickness
V	velocity
w	fin thickness at root
X_{cp}	distance to the center of pressure measured from base along the axis of symmetry

X_{cg}	distance to the center of gravity measured from base along the axis of symmetry
x	distance aft of nose tip or fin leading edge flutter parameter
y	span distance from root of fin
y_1	span distance from rocket axis
$\bar{y}$	centroid distance from rocket axis
α	angle of attack
$\bar{\alpha}$	total angle of attack ($\Delta\omega = 0$)
β	angle of yaw
δa	aerodynamic misalignment
δ_F	thrust misalignment
δ_f	fin-cant angle
ϵ	emissivity
Λ	fin sweepback angle
λ_o	nonrolling damping constant
$\Delta\lambda$	damping constant due to roll
ρ	density
ω_o	pitching frequency
$\Delta\omega$	rolling frequency

Subscripts

b	body alone
b+f	body with fins
c	composite
f	fin
n	nose cone

ARCHER DESCRIPTION

An assembly drawing, photograph and specifications of the Archer vehicle are shown in Figures 1, 1-A and Table 1, respectively. Total length of the rocket is 133.45 inches (19.06 calibers) and the fin span is 24.5 inches (3.5 calibers). Total weight of the rocket excluding payload is approximately 294 pounds. Vehicle center of gravity, transverse and axial

moments of inertia as functions of time are plotted in Figures 2, 3 and 4.

A nose-cone drawing and photograph appear in Figures 5 and 5-A, respectively. The nose cone was manufactured of fiberglas with an ablative layer of epoxypolysulfide. The nose cone is unpressurized and it is planned to jettison it near apogee, exposing the instrument package. This will be accomplished by means of a timer and heavy spring arrangement. The nose cone, a minimum drag secant ogive with a hemispherical tip, is 28.7 inches long and has a 0.200 inch thick wall composed of 0.100 inch fiberglas and a surface coating of 0.100 inch epoxypolysulfide. Total weight of the nose cone is 4.37 pounds. The volume available for instrumentation inside the nose cone is roughly that of a cone frustrum whose length is 18 inches and whose major and minor diameters are 6.810 and 3.675 inches, respectively. An additional 10-inch cylindrical section is being added to the nose cone by the Naval Missile Center, Pt. Mugu, California, to make room for additional instrumentation peculiar to the test firings. This addition will not, however, appear in any Archer production rockets.

A drawing of the Archer engine is shown in Figure 6 while the operating parameters are listed in Table 2. The motor is 106 inches long and 7 inches in diameter, with the case, head and nozzle shells made of heat-treated steel. It operates at an average internal pressure of 1200 psi and develops an average sea-level thrust of 1375 pounds over a 35 second burning time (Figure 7). Total impulse is 48,000 pound-seconds. The propellant grain is cast of Arcite 427-B, an aluminized plastisol propellant. The engine center of gravity as a function of time is shown in Figure 8.

The case is insulated from the propellant flame by the use of a molded-in-place, 41-RPD asbestos-phenolic liner. The molded-in-place liner has the advantage of conforming to the inside surface of the motor and thus eliminating any voids and irregularities. The pressure molding of the liner leaves the liner in the motor under a slight compression, reducing the required physical properties to withstand radial deformation under motor pressurization.

The Archer rocket nozzle is of a lightweight design featuring the most advanced materials know-how available. The insert is made of high density graphite, "ZTA," manufactured by the National Carbon Company. The insert and "ATJ" graphite exit cone are insulated from the steel nozzle shell by zirconia-phosphate materials, while the nozzle entrance section is insulated with Guardian I Compound developed by the ARC.

A fin drawing and photograph appear in Figures 9 and 9-A, respectively. The fins were built-up, rather than being made of solid material in order to keep the weight down. In cross section, the fins are straight panels with wedge-shaped leading and trailing edges. The planform includes a 60° swept leading edge with a perpendicular trailing edge. Subsequent production fins, depending on the difficulty of manufacture, might include a double convex cross section and a swept trailing edge. The fins are made of 0.075 inch thick magnesium skin with an ablative coating of epoxypolysulfide and include a 0.015 inch thick stainless steel cuff to protect the leading edge from aerodynamic heating. Fin blade span is 8.750 inches, root-chord 22.625 inches, and the fin tapers from 0.500 inch at the base to 0.150 inch at the tip. The total weight of four fins is approximately 10 pounds.

AERODYNAMIC DESIGN

The four-caliber-long secant-ogive nose cone was used because it fulfilled the instrumentation volume requirement as well as the requirement for a low drag contour. Fiberglas was decided upon as a suitable material to meet the following needs: (1) to allow instrumentation signals to pass through the skin, (2) to be structurally strong, (3) to be light and (4) to withstand reasonable aerodynamic heating. Subsequent detailed aerothermodynamic studies indicated higher heating rates than had been originally anticipated, resulting in a marginal condition. This was remedied by the application of a surface layer of epoxypolysulfide which ablates at high temperatures and keeps the temperature of the fiberglas low enough to maintain its structural integrity. Another modification to the original design was the replacement of a solid aluminum nose-cone tip with a solid fiberglas hemispherical nose tip. This change was also made due to aerodynamic heating considerations. The final nose-cone design is shown in Figures 5 and 5-A. Detailed discussions relating to nose-cone aerodynamic heating, loads and structural design and manufacture are treated in later sections.

The next item to be determined was the fin design. It was concluded that a cruciform arrangement with a minimum static margin of two calibers would provide adequate static stability for the Archer sounding rocket. This design criterion was applied at burnout conditions which are considered the most critical. Burnout conditions were obtained from preliminary vertical trajectory calculations using the Iris drag curve and estimated weight of the total vehicle configuration which resulted in the following conditions at the design point:

$V = 5950$ ft/sec
$h = 85{,}000$ ft
$M = V/a = 6.13$

Determination of the fin area based on the conditions mentioned above was accomplished in the following manner:

The criterion for adequate static stability has been stated:

$$\frac{X_{cg} - X_{cp}}{d} \geq 2 \tag{1}$$

The center of gravity, X_{cg}, of the vehicle was calculated to be, based on the engine center of gravity and probable weight of the components, approximately 8.5 calibers from the base.

The center of pressure is expressed by:

$$X_{cp} = \frac{(C_{L_\alpha})_b (X_{cp})_b + (C_{L_\alpha})_f (X_{cp})_f}{(C_{L_\alpha})_b + (C_{L_\alpha})_f} \tag{2}$$

The body lift-curve slope, $(C_{L_\alpha})_b$, was obtained by the extrapolation of wind-tunnel data from similar aerodynamic shapes. This yielded a value of $(C_{L_\alpha})_b = 2.56/\text{rad}$.

Similarly, the body center of pressure, $(X_{cp})_b$, was obtained from the same data and calculated to be approximately 15.5 calibers from the base.

The fin center of pressure was determined to be about one caliber from the base.

Combining equations (1) and (2), the stability criterion becomes:

$$(C_{L_\alpha})_f = (C_{L_\alpha})_b \left[\frac{\frac{(X_{cp})_b}{d} - \left(\frac{X_{cg}}{d} - 2 \right)}{\left(\frac{X_{cg}}{d} - 2 \right) - \frac{(X_{cp})_f}{d}} \right] \tag{3}$$

and when the above values are used,

$$(C_{L_\alpha})_f = 4.20/\text{rad} \tag{3a}$$

It was then decided to use two-dimensional theory to establish the lift-curve slope of the fins. This method is based on the assumption that the unfavorable effects of tip losses will be balanced by the favorable effects of body upwash. This same analysis, used for the Iris Sounding Rocket (reference (3)), was quite accurate in predicting the wind-tunnel results for Iris as given in reference (4). According to the above, we write (e.g., 5):

$$(C_{L_\alpha})_f = \frac{A_f}{A_b} \frac{4 \cos \Lambda}{\sqrt{M^2 \cos^2 \Lambda - 1}} \tag{4}$$

where A_f is the projected area of two fins.

After consideration of the Mach line at the design Mach number, it was decided to sweep the leading edge of the fins a total of 60 degrees, Λ, from the vertical. Now equations (3a) and (4), together with the design Mach number, require that the planform area of each fin be:

$$\frac{A_f}{2} \geq 0.81 \text{ ft}^2 \tag{5}$$

This was the area used to design a one-caliber-span fin panel which yielded a total fin span of three calibers. Subsequently, it was suggested by the ARC that the span be increased somewhat as an added protection against blanketing effects. Since there was no mechanical restriction against increasing the span, 0.25 caliber was added to each panel. This made the final area close to a square foot per panel and the total fin span 3.5 calibers. The preceding considerations resulted in the fin design shown in Figures 9 and 9-A. Finally, a coating of epoxypolysulfide was applied to the fin panels as an added protection against aerodynamic heating. Detailed discussions relating to fin aerodynamic heating, loads and structural design and manufacture are treated in later sections.

STATIC STABILITY

A 1/10th scale model, Figure 10, of the Archer Sounding Rocket was designed and built at the NOL for wind-tunnel testing to determine the static stability characteristics of

the vehicle. It will be noted that the very tip of the model nose is a cone, as was prescribed in the original design. The final version of the Archer sounding rocket nose cone incorporates a hemispherical tip which was included for aerodynamic heating reasons. It is believed that this detail, when scaled down, would not yield appreciably different static stability characteristics. This report includes the results obtained from these investigations conducted in Supersonic Tunnel No. 1 at Mach numbers of 0.49, 0.93, 1.03, 1.52, 2.28, 3.25, 4.14 and 4.85.

A two-component internal strain-gage balance system (reference (6)) designed and built at the NOL was used in obtaining the aerodynamic forces and moments acting on this configuration. The test conditions are listed in Table 3. Data were taken at angles of attack ranging from -5 to +20 degrees for each Mach number tested. In addition, schlieren photographs using a 1/100th of a second exposure time and a tungsten light source were taken during the tests to provide information on the flow characteristics peculiar to the vehicle. Figure 11 contains representative schlieren photographs of the model configuration taken at zero and 10 degrees angle of attack for Mach number 1.52.

Strain-gage data were reduced to lift force and pitching moment coefficients according to standard aerodynamic convention and, subsequently, the slopes of these data (Figures 12 through 14) through zero degrees angle of attack were determined and used in the calculations which appear in this report.

All the aerodynamic coefficients were based on body cross-sectional area and the burnout center of gravity was used as the moment reference center for the data reduction. A positive pitching moment is designated as an overturning moment when the model is at a positive angle of attack.

Figure 15 is a plot of the estimated pitch-damping-moment coefficient, based on wind-tunnel measurements of similar configurations, as a function of Mach number.

Figures 16 and 17 show the vehicle lift-curve slope and static-stability margin as a function of time, respectively. It is interesting to note that the minimum static-stability margin occurs at burnout and is equal to approximately 3.75 calibers. This exceeds the design criterion and is due, in part, to the subsequent lengthening of the total fin span from 3 to 3.5 calibers. Further, it is gratifying to note a static-stability margin of approximately 5 calibers when the vehicle is expected to pass through pitch-roll resonance which occurs at approximately 26 seconds of flight time. This is, perhaps,

the most critical portion of the flight at which time a good margin of static stability tends to keep the rocket from assuming high angles of attack and its attendant side forces at the asymmetrical roll positions. Increased side force is of importance when the pitch frequency of the vehicle is equal to its roll frequency because a condition termed "lunar motion" may arise. During this flight condition, the same side of the vehicle always faces inward for any angle of attack and large yaw angles may result (reference (7)). The method by which the difficulties associated with pitch-roll resonance are to be avoided in the present design is discussed in the following section which deals with dynamic stability.

The drag coefficient curve which appears in Figure 18 is the one determined for the Iris sounding rocket during its design and development program. Due to the difficulty of establishing a drag curve for a burning rocket, it was felt that advantage should be taken of the existing drag data for the Iris which is aerodynamically similar to the Archer. It has been assumed that the drag coefficients for Iris and Archer are the same. Further, it was reasoned that any differences in drag coefficients which might exist between the two configurations would, in all probability, be of the same order as the error introduced in establishing a completely new drag curve. Consequently, with an available drag curve a savings in time was realized by the immediate ability to make calculations necessary for the preliminary design.

DYNAMIC STABILITY

Dynamic stability calculations were concerned primarily with the avoidance of pitch-roll coupling. Specifically, this involved the determination of the natural pitch frequency of the vehicle and subsequently the calculation of roll programs[1] which would cross over the descending side of the pitching frequency curve prior to engine burnout (Figure 19). This type of roll build-up affords a single point cross-over as opposed to the possibility of the roll rate following the pitching rate upward on the ascending portion of the curve with its consequent resonance problems. Three roll programs, all such that they crossed on the descending side of the pitching frequency curve, were determined and examined in the light of other considerations such as magnification factors, alignment problems, etc. As a consequence, a fin incidence angle of 15 minutes, which appeared to be optimum, was selected. As shown on Figure 19, this fixed the cross-over point at approximately 3.15 cycles per second at a flight time of about 26 seconds.

---

[1] fin-cant angles which provided specific roll rates at specific flight times

The pitching frequency of the Archer configuration was calculated according to the following equation:

$$\omega_0 = \frac{1}{2\pi}\sqrt{\frac{\rho V^2 A_b d}{2I}\, C_{M_\alpha}} \tag{6}$$

using the nominal trajectory data shown in Table 8 and plotted in Figures 20 and 21. In general, the natural frequency expression contains damping terms, rolling velocity and longitudinal acceleration; however, for a first approximation the above expression was considered adequate.

The fin-cant angle required to produce the design roll rate of 3.15 cycles per second was determined using the dynamics equation for rolling moment, neglecting roll damping terms and correcting $\Delta\omega$ by assuming a 15 percent loss in roll rate due to damping. This was accomplished by taking the following equation:

$$I(\dot{\Delta\omega}) - 4\int y_f \frac{\Delta\omega}{V} C_{\ell_\alpha} q c\, y_f\, dy_f + 4\int \delta_f C_{\ell_\alpha} q c\, y_f\, dy = 0 \tag{7}$$

and assuming (C_{ℓ_α}) to be constant over the entire fin and making the simplifying assumption that $\frac{I_x(\dot{\Delta\omega})}{4 C_{\ell_\alpha} q} << 1$.

Equation (7) then reduces to:

$$\int \frac{(\Delta\omega)}{V} y_f^2\, c\, dy_f = \int \delta_f\, y_f\, c\, dy_f \tag{8}$$

and

$$\frac{\Delta\omega}{V}\int y_f^2\, dA = \delta_f \int y_f\, dA \tag{9}$$

Then by definition the following equation results:

$$\frac{\Delta\omega}{V} I_f = \delta_f \bar{y} \frac{A_f}{2} \tag{10}$$

and solving equation (10) for fin-cant angle yields:

$$\delta_f = \frac{\Delta\omega I_f}{V\bar{y}\frac{A_f}{2}} \tag{11}$$

AERODYNAMIC LOADS

In order to determine the maximum loads encountered by the rocket nose cone and fin assembly, it was necessary to predict the angle of attack history of the flight. The total angles of attack ($\Delta\omega$=0) resulting from the estimated misalignments (Figure 22) were computed. Also, the trim magnification factors in the region of pitch-roll resonance were computed for three fin-cant angles. The total angle of attack at zero roll rate multiplied by this magnification factor gives the total angle of attack with roll.

A study of the equations of motion indicated that, if rolling and damping terms were neglected, the total angle of attack ($\Delta\omega = 0$) expression reduced to the following moment equation:

$$F_{SL} X_{cg} \delta_F - \frac{1}{2} \rho V^2 A_b d C_{M_\alpha} (\bar{\alpha} - \delta_\alpha) = 0 \tag{12}$$

(see Figure 22 for notation). It was felt that this simplification was permissible for estimation purposes, particularly since the omission of damping terms gave conservative answers from a structural design standpoint. Figure 23 shows the total angle of attack ($\Delta\omega = 0$), α, computed from equation (12).

The equations for the magnification factor (reference (8)) are relatively complex for the general case; however, for the Archer configuration they may be simplified by making the following assumptions:

a. Axial moment of inertia I_x << transverse moment of inertia I

b. Damping constant due to roll $\Delta\lambda$ << non-rolling constant λ_o

c. Rolling velocity $d\Delta\omega$ << flight velocity V

Consequently, the magnification factor is:

$$f = \frac{1 - \left(\frac{\lambda_o}{\omega_o}\right)^2}{\sqrt{\left[\left(\frac{\lambda_o}{\omega_o}\right)^2 + \left(1 + \frac{\Delta\omega}{\omega_o}\right)^2\right]\left[\left(\frac{\lambda_o}{\omega_o}\right)^2 + \left(1 - \frac{\Delta\omega}{\omega_o}\right)^2\right]}} \qquad (13)$$

This expression may be reduced further since $\left(\frac{\lambda_o}{\omega_o}\right)^2 \ll 1$

$$\text{then } f = \left[\left(1 + \frac{\Delta\omega}{\omega_o}\right)\sqrt{\left(\frac{\lambda_o}{\omega_o}\right)^2 + \left(1 - \frac{\Delta\omega}{\omega_o}\right)^2}\right]^{-1} \qquad (14)$$

The ratio of roll to pitch frequency, $\frac{\Delta\omega}{\omega_o}$, in the region of interest, is approximately equal to one. Using the same assumptions as discussed above, the expression for $\frac{\lambda_o}{\omega_o}$ (reference (8)) reduces to:

$$\frac{\lambda_o}{\omega_o} = \frac{-\sqrt{2}\left[1 - \frac{1}{2(k/d)^2}\left(\frac{C_{M_q}}{C_{N_\alpha}}\right)\right]}{\sqrt{-4\frac{C_{M_\alpha}/C_{N_\alpha}}{\frac{C_{N_\alpha}}{4m/\rho A_b d}(k/d)^2}}} \qquad (15)$$

In the solution of equation (15), it was assumed that $C_{N_\alpha} \simeq C_{L_\alpha} + C_D$.

Figure 24 shows the magnification factor for the three roll programs considered. Figure 25 shows the resulting total angle of attack($\Delta\omega \neq 0$), $f\bar{\alpha}$, for the three roll rates. The equations used to determine the nose cone and fin loads were, respectively:

$$P_n = q A_b \left(C_{L_\alpha}\right)_b f\bar{\alpha} \qquad (16)$$

$$P_f = \frac{1}{2} q A_b \left(C_{L_\alpha}\right)_f f\bar{\alpha} \quad \text{(for one fin)} \tag{17}$$

The lift-force slopes used for the nose-cone load calculations were those for the body alone configuration. This afforded a conservative estimate for design purposes. Figures 26 and 27 indicate the loads obtained for the three roll rates investigated. As indicated on the plots, the maximum loads obtained for the crossover point selected (26 seconds of elapsed flight time) were 325 and 620 pounds for the nose cone and fins, respectively.

AERODYNAMIC HEATING

Aerodynamic heating calculations were performed at the NOL using a program involving numerical approximations as described in reference (9). The solutions took the form of a time history of temperature distribution. Local Mach numbers and pressures were used and the Reynolds number of transition was set at one million. The Archer trajectory, Table 8, and ambient atmosphere were specified.

Results of the nose-cone heating calculations are shown in Figure 28. The temperature histories plotted are for a 0.150 inch thick fiberglas wall at an axial station 2.5 feet from the nose. At this station the nose-cone wall was divided, through the wall, into three elements of 0.030, 0.090 and 0.030 inches and the temperature calculated at the center of each element as a function of time. This was considered a critical area, being in the approximate region of the nose-cone juncture with the rocket-motor casing. Table 4 specifies the nose-cone material and its thermal characteristics.

In addition to the above machine calculations which indicated surface temperatures approaching 1500° R, a hand calculation (reference (10)) indicated that the maximum stagnation point temperature might reach 2500° R. These calculations, which indicated higher heating rates than had been originally anticipated, showed that the nose-cone design was marginal from the standpoint of aerodynamic heating. It was reasoned that the temperatures were conservatively high because ablation would certainly occur, but just how much cooling would be realized from this ablation and how much fiberglas material would be left intact were questionable. It was concluded, therefore, that additional studies would be needed in order to determine the effect of this ablation and whether special ablative coatings to the fiberglas would be necessary. The Missiles and Space Vehicle Department of the General Electric Company, Philadelphia, Pa., was asked to investigate the

severity of the ablation and temperature problem using the 0.150 inch thick fiberglas material specified in Table 4. The specifications were that at least 0.050 inch thick wall of the initial fiberglas nose cone should be maintained at a temperature (760° R) sufficiently low so as to provide structural integrity. The time schedule required that GE investigate concurrently the possibility of applying a special ablative coating to the nose cone in the event the 0.150 inch thick fiberglas material proved unsatisfactory.

The GE ablation and temperature calculations were accomplished using a one-dimensional conduction solution with surface melting. The first group of calculations was performed using the fiberglas thermal properties as specified by NOL with a parametric variation of melting temperature (1000 to 1400° R). The results of these calculations all indicated that the original 0.150 inch thick fiberglas nose cone would be adequate. The data of Figure 29 are typical of these results and show the thermal response of the nose cone using a melting temperature of 1200° R. While the above results appeared to be satisfactory, GE made an additional computation using what they estimated to be the correct thermal conductivity for a highly glass-filled plastic. These results, again for a melting temperature of 1200° R, are shown in Figure 30. In this case, it is noted that some high temperature difficulties will occur, and that the temperature limit of 760° R at the 0.10 inch depth will be exceeded.

Concurrent with the above, GE computed the thermal response of the fiberglas nose cone when coated with various thicknesses of epoxypolysulfide using the NOL fiberglas conductivity value. The k, ρ and C_p for epoxypolysulfide are approximately equal to 3×10^{-4} Btu/ft-sec° R, 79 lb/ft^3 and 0.45 Btu/lb° R, respectively. All of these configurations provided adequate protection. A final computation was then made with a near optimum configuration of 0.10 inch epoxypolysulfide over 0.10 inch of fiberglas using the GE estimated conductivity for the fiberglas. This result is shown in Figure 31. The final soak temperature is estimated to be less than 700° R.

As a result of these studies, it was decided to approach the problem conservatively and to modify the nose cones to include a 0.10 inch thickness of fiberglas coated with a 0.10 inch thickness of epoxypolysulfide. The ablative coating was developed and applied by GE. Further, to retard heat conduction to the main body of the nose cone, NOL changed the nose-cone tip from a solid aluminum cone to a solid plastic hemisphere.

The heat-transfer program of reference (9) was also applied to the Archer fins, using the thermal characteristics specified in Table 5, and the results are shown in Figure 32.

Included in this figure is a plot of the tensile yield strength of the magnesium fin material. Again, the strength appears somewhat marginal due to aerodynamic heating. Fortunately, the maximum aerodynamic loads are experienced early in the flight regime when the tensile strength is high. Nevertheless, it was decided to apply a coating of epoxypolysulfide to the existing fins and assembly as an added safety precaution. This coating is particularly important in the region of fin attachment where the mounting bracket and bolts are exposed to the aerodynamic heating. The leading edge of the fin is protected by a 0.015 inch thick stainless steel cuff.

STRUCTURAL DESIGN AND MANUFACTURE OF COMPONENTS

The Archer nose cone consists of a solid tip, with a 0.723 inch radius, threaded to an ogive fairing which encloses the instrumentation package.

The nose tip is a plastic material, Fiberite MX-6500, produced by Fiberite Molding Products Incorporated, Winona, Minnesota, which has an ablation temperature of approximately 3500° F.

The ogive fairing is an epoxy-base, glass-phenolic material which was manufactured by helically winding continuous-length glass fibers, coated with liquid epoxy over an aluminum mandrel. The completed winding was cured, then machined to a uniform 0.100 inch thickness. The fairing was then covered with an ablative coating which was discussed previously.

A nose-cone load of 325 pounds was obtained from the data of Figure 26. This load was assumed to act at 27.25 inches from the juncture between the nose and motor tube. Such an assumption resulted in conservative structural estimates. Stresses in the fiberglas (see Table 6) were computed, assuming no load would be carried by the ablative coating, according to the following equation:

$$s = \frac{P(\ell d_o/2)}{\frac{\pi}{64}(d_o^4 - d_i^4)} = 2236 \text{ lb/in}^2 \qquad (18)$$

The nose cone is held against a shoulder on the motor head plate by a structure, passing through the instrument section, which attaches between a point on the nose near the front (see Figure 5) and the head plate.

With the nose attached to the motor through compression only, it was necessary to apply pre-load which produced stresses

equal to or greater than the stress due to the aerodynamic loads in order to prevent separation. Consequently, the stresses in the fiberglas amounted to 2236 x 2 = 4472 lb/in^2. The pre-load necessary was:

$$P = 2236 \frac{\pi}{4} (d_o^2 - d_i^2) = 4821 \text{ lb} \tag{19}$$

The pre-load of equation (19) produced compressive stress throughout the nose cone with the maximum being near the front end where the area is minimum.

$$s = \frac{P}{\frac{\pi}{4} (d_o'^2 - d_i'^2)} = 9442 \text{ lb/in}^2 \tag{20}$$

The point considered most critical in the nose support structure was the explosive bolt which will be fired to release the nose cone. This bolt was loaded in tension and must carry both the pre-load and aerodynamic loads. Thus the load calculated was:

$$P = \frac{M}{d_o/2} + \text{PRE-LOAD} = 7247 \text{ lb} \tag{21}$$

The explosive bolt used, Holex, Inc. part no. 2508-14, will support a tensile load of 14,000 pounds.

The Archer fin (Figure 9) was fabricated from a magnesium alloy (Dow Chemical Co. HK 31A-H24) which maintains good strength properties at elevated temperatures (see Table 7). The structure consists of a solid base bar and solid leading and trailing edge struts. A thin skin (0.075 inch thick) was welded to the front and trailing edge struts, then riveted to the base bar. Two stiffeners were sandwiched between and riveted to the outer skins to distribute the load between the sides. The leading edge strut was covered by a thin (0.015 inch thick) stainless steel sheet for heat protection. This cover was riveted to the leading edge strut.

Flutter safety estimates were made using an empirical method described in reference (11). This method was determined from samplings of a large amount of experimental data. It divides

the configurations into safe and unsafe groups based on the following parameters: torsional stiffness, taper ratio, aspect ratio, thickness ratio and pressure. The above parameters for the Archer fin configuration (Figure 9) were:

a. Taper ratio, $\frac{L_t}{L_r} = 0.330$

b. Aspect ratio, $\frac{b^2}{A_f/2} = 0.581$

c. Shear modulus = 2.42×10^6 lb/in^2 for magnesium

From these values and the graph of reference (11),

$$\frac{p}{p_o}\left(\frac{\frac{L_t}{L_r}+1}{2}\right)x = 0.7 \qquad (22)$$

Letting $\frac{p}{p_o} = 1$ which was the most severe condition possible, $x = 1.053$. Again from graphs of reference (11), this value of x required a thickness ratio of 0.015. A 1.50 safety factor was added, and the required root thickness became: 1.50 x 0.015 x 22.625 = 0.498 inch. For convenience this value was rounded off to 0.500 inch fin root thickness.

Strength calculations were based on a fin load of 620 pounds (Figure 27) which was assumed to be equally distributed over the fin surface.

Thus the pressure, $p = \frac{p_f}{A_f/2}$, amounted to 4.68 pounds per square inch.

The symbols used in the following analytical expression for the bending moment are included in Figure 9.

$$M = \int_0^H p\left(L_t + \frac{H-y}{\tan\Lambda}\right)y\,dy = \frac{p}{\tan\Lambda}\left[\frac{L_t H^2}{2}\tan\Lambda + \frac{H^3}{6}\right] = 2239 \text{ in-lb} \qquad (23)$$

It was conservatively assumed that the two side plates carried the entire fin bending load and that this load reacted as

tension and compression in these members. The stresses developed were as follows (see Figure 9):

$$s = \frac{\frac{M}{2(w-t)}}{\ell t} = 2431 \text{ lb/in}^2 \qquad (24)$$

If instead of the previous assumption we consider the fin as a beam in bending:

$$s = \frac{Mc}{I} = \frac{M\frac{w}{2}}{\frac{\ell}{12}\left[w^3-(w-2t)^3\right]} = 5654 \text{ lb/in}^2 \qquad (25)$$

Bending stresses in the fin mounting lugs were calculated from the expression:

$$s = \frac{M\left(e-\frac{w}{2}\right)}{6e}\left(\frac{C}{I}\right) = 15{,}000 \text{ lb/in}^2 \qquad (26)$$

At the time in flight that this maximum bending load occurs, loads due to drag and acceleration are low and may be neglected.

The tension load on the 1/4-inch 28-NF fin mounting screws was based on the tension load resulting from the predicted aerodynamic loads plus the load due to a 10 inch-pound torque used in setting the fins and is:

$$\text{tension} = \frac{M}{6e} + \text{pre-load} = 821 \text{ pounds} \qquad (27)$$

The allowable tensile load is 5500 pounds for Allen cap screws.

Fin band stress was calculated based on the band carrying tension only, thus:

$$s = \frac{\frac{M}{6e}}{0.75 \times 0.062} = 11{,}852 \text{ lb/in}^2 \qquad (28)$$

where the 0.75 inch and 0.062 inch were band width and thickness, respectively. The fin bands are clamped to the motor casing with No. 6-40NF (two per band) Allen cap screws torqued to 5 inch-pounds. The tension force in these screws was:

$$P = \frac{M}{6e(2)} + \text{pre-load} = 509 \text{ pounds} \qquad (29)$$

The allowable yield load for these screws is 1500 pounds per screw.

TRAJECTORY AND DISPERSION ANALYSIS DATA

All of the trajectories for Archer were calculated under the assumptions of a rigid body model through sustainer burnout and a particle model thereafter until impact. Rigid body trajectory calculations were based on the aerodynamic coefficients determined from wind-tunnel tests mentioned previously in this report. Due to the small roll rate, aerodynamic coefficients associated with rolling motion were neglected and the pitch-damping-moment coefficient was estimated (Figure 15). The nominal trajectory variables are listed as functions of time in Table 8. This table includes velocity, altitude, ground range, flight-path angle, acceleration and gross weight at 10-second time intervals and at burnout. The altitude and velocity as well as Mach number are plotted as functions of time in Figures 20 and 21, respectively. In addition, the dynamic pressure as a function of time is presented in Figure 33.

Table 9 lists the effects of Q.E. as well as head, tail and cross winds on burnout altitude, burnout range, maximum altitude, impact range and impact cross range.

Wind-weighting factors as a function of altitude layer are presented in Table 10. The wind-weighting factors were determined for range winds and were assumed to be valid for cross winds. This assumption appears to be reasonable based on other published results. Table 10 also contains unit wind effects in feet of deflection per ft/sec of ballistic tail, head and cross wind, respectively, as well as the Q.E. and azimuth corrections for range winds and cross winds in degrees per ft/sec of ballistic wind. All negative signs in Table 10 indicate deflections opposite to the wind direction.

Table 11 lists five major causes of dispersion and the resulting deflection to the normal impact point caused by a 2σ and 3σ variation of these causes. In four cases these quantities

were estimated and are so marked in the table. The remainder of the data was determined directly from the trajectory results. In every case the deflection data are conservative. The quantity described as "launch errors and malalignments" includes the effects of tip-off, thrust malalignment, fin malalignment and other possible sources of angular error. At the bottom of Table 11 are the total dispersion data which are simply the square roots of the sum of the squares of the individual deflections.

CONCLUSIONS

An initial design of the Archer nose cone and fins was accomplished on the basis of preliminary vertical trajectory calculations. Subsequently, refinements to the original design were made on the basis of final trajectory calculations using Archer wind-tunnel data. This led to the following design conclusions:

a. Static stability, used as the design criterion, was minimum at burnout with the center of pressure being 3.75 calibers aft of the center of gravity.

b. Dynamic stability calculations, concerned primarily with the avoidance of pitch-roll coupling, indicated that a fin-cant angle of 15 minutes appeared to be the optimum and would cause the vehicle to pass through resonance at approximately 3.15 cycles per second and 26 seconds of flight time.

c. Aerodynamic loads based on the aerodynamic coefficients obtained from the NOL wind-tunnel tests in conjunction with predicted total angles of attack ($\Delta\omega \neq 0$), neglected the aerodynamic damping terms and are considered conservative.

d. Aerodynamic heating calculations, including the effects of ablation, were performed on the fiberglas nose cone. These indicated a marginal condition which was corrected by modifying the nose cone to include an outside layer of epoxy-polysulfide. The ablation of this material will protect the structural integrity of the fiberglas which requires the maintenance of at least 0.050 inches wall at no higher temperature than 760° R.

Heating calculations on the fins indicated rather high temperatures and as a safety precaution, epoxypolysulfide was also applied to the fins and mounting assembly.

e. Structural design was based on aerodynamic loads encountered at resonance, and the minimum structural safety factor was 1.3 for the fin mounting lugs. This factor was based on the allowable material strength at 435° F. With the

epoxypolysulfide coating on the fins, the mounting lugs should not reach 435° F at the point of maximum loads.

f. Final trajectory calculations, based on wind-tunnel data, indicated the feasibility of the present system to attain altitudes in the vicinity of 100 miles with a quadrant elevation of 80 degrees.

REFERENCES

(1) Work Request, No. WR-2-000035 from NRL to NOL of 3 Oct 1961

(2) Grey, J., "Aerodynamic Design and Performance Study of the Iris Sounding Rocket," Parts 1 and 2, Greyrad Corp., Livingston, N. J., Reports ARC-11 and 12, 1960

(3) Grey, J., "Second Interim Report of the Preliminary Aerodynamic Design of the Iris Sounding Rocket and Addendum," Greyrad Report ARC-6, Atlantic Research Corp., 1958

(4) Glover, J.H., "Supersonic Wind-Tunnel Investigation of 14.511-Inch Iris Model," Atlantic Research Corp., 1959

(5) Shapiro, A.H., "The Dynamics and Thermodynamics of Compressible Fluid Flow," Vol. I, Ronald Press, N. Y., Chapter 14, 1953

(6) Shantz, I., Gilbert, B.D., & White, C.E., "NOL Wind-Tunnel Internal Strain-Gage Balance System," NAVORD Report 2972, 1953

(7) Nicolaides, J. D., "An Hypothesis for Catastrophic Yaw," BUORD Ballistic Technical Note Number 18

(8) Nelson, R.L., "The Motions of Rolling Symmetrical Missiles Referred to a Body Axes System," NACA TN 3737, 1956

(9) Fox, D.W., Shaw, H., Jr., Jellinek, J., "Numerical Approximations in Heat Transfer Problems and Usage of IBM 7090 Computer for Solutions," Applied Physics Laboratory, The Johns Hopkins University Report CF-2954, 1962

(10) Truit, R.W., "Fundamentals of Aerodynamic Heating," Ronald Press, N. Y., 1960

(11) Martin, D.J., "Summary of Flutter Experiences as a Guide to the Preliminary Design of Lifting Surfaces on Missiles," NACA Conference on Aerodynamic Design Problems of Supersonic Guided Missiles, Oct 1951

TABLE 1

ARCHER PHYSICAL CHARACTERISTICS

1.	Nose cone	
	length	28.700 in
	major diameter	7.300 in
	wall thickness	0.200 in
	weight	4.37 lb
2.	Forward head	
	weight	5.05 lb
3.	Motor tube	
	length	100.50 in
	nominal diameter	7.00 in
	wall thickness	0.050 in
	weight	38.30 lb
4.	Insulation liner	
	length	97.5 in
	major diameter	6.90 in
	weight	16.23 lb
5.	Propellant grain	
	length	97.5 in
	propellant weight	200.0 lb
	inhibitor weight	7.91 lb
	total weight	207.91 lb
6.	Nozzle assembly	
	length	7.25 in
	weight	10.50 lb
7.	Fins	
	weight (per set)	10.00 lb

TABLE 1

ARCHER PHYSICAL CHARACTERISTICS

8. Nozzle cover	
weight	0.976 lb
9. Igniter	
weight	0.50 lb
Total unit weight excluding payload	293.836 lb

TABLE 2

ARCHER OPERATING PARAMETERS

1.	Chamber pressure	1200 lb/in^2
2.	Throat area	0.630 in^2
3.	Throat diameter	0.900 in
4.	Average thrust	1375 lb
5.	Burning time	35.0 sec
6.	Total impulse	48,000 lb-sec
7.	Expansion ratio	10/1
8.	Expansion to	14.7 lb/in^2

TABLE 3

WIND-TUNNEL RUNS AND TEST CONDITIONS

Run	M	Configuration	q(lb/in^2)	Re x 10^{-6}
1	0.485	body alone	2.10	3.98
2		body with fins		
3	0.925	body with fins	4.85	5.60
4		body alone		
5	1.026	body alone	5.30	5.77
6		body with fins		
7	1.52	body with fins	6.05	5.75
8		body alone		
9	2.28	body alone	4.40	4.32
10		body with fins		
11	3.25	body with fins	2.05	2.79
12		body alone		
13	4.14	body alone	1.02	1.85
14		body with fins		
15	4.85	body with fins	0.45	1.35
16		body alone		

TABLE 4

THERMAL CHARACTERISTICS OF NOSE CONE

Material: Fiberglas (Union Carbide Corp.)

1. Resin--Epoxy ERLA 2256
2. Glass type E
3. Contents by weight: 60% glass--38% resin--2% colloidal silica
4. Curing system 0820-28 PHR

Thermal Characteristics:

1. Thermal conductivity (k)

Temperature (°R)	*k x 10^5 (BTU/ft-sec °R)
500	2.45
600	2.72
700	2.95
1000	3.67
1200	4.12

2. Thermal capacitance (ρc_p)

   33.8 Btu/ft^3 °R--constant for the temperature range 375--1020 °R

3. Density (ρ)--112.5 lb/ft^3
4. Emissivity value (ϵ)--.80

* The GE value for k is 7×10^{-5} and is considered constant with temperature.

TABLE 5

THERMAL CHARACTERISTICS OF FIN

Material: Magnesium--HK 31A-H24 (Dow Metal Products Co.)

1. Composition:

Thorium	2.5--4.0%
Zirconium	.45--1.0%
Manganese	.15% maximum
Total impurities	.30% maximum

Thermal characteristics:

1. Thermal conductivity (k)

Temperature (°R)	k (BTU/ft-sec °R)
500	.0183
700	.0185
900	.0188

2. Thermal capacitance (ρc_p)

Temperature (°R)	ρc_p (BTU/ft^3 °R)
460	27.0
660	28.7
860	30.4

3. Density (ρ)--112.5 lb/ft^3

4. Emissivity value (ϵ)--.20

TABLE 6

MAXIMUM LOADS AND STRESSES IN NOSE FAIRING AND ATTACHMENTS

Item	Mat'l	Max Stress (lb/in^2)	Max Load (lbs)	Allowable Stress (lb/in^2)	Allowable Load (lbs)
1. Nose fairing (at base)	Epoxy-glass	4472	--	17,500	--
2. Nose fairing (front end)	Epoxy-glass	9442	--	17,500	--
3. Explosive bolt	see note	--	7247	--	14,000

Note: Holex Inc., 2751 San Juan Rd., Hollister, Calif.--Part No. 2508-14

TABLE 7

MAXIMUM LOADS AND STRESSES IN FIN AND ATTACHMENTS

Item	Material	Max Stress (lb/in^2)	Max Load (lbs)	Allowable Stress (lb/in^2)	Allowable Load (lbs)
1. Fin skin	Magnesium	5,654	--	19,500*	--
2. Mounting lugs	Magnesium	15,000	--	19,500*	--
3. Fin bands	Steel SAE 4140	11,852	--	150,000	--
4. Mounting screws	Allen Cap Screws (1/4"-28NF)	--	821	--	5,500
5. Fin band screws	Allen Cap Screws (6-32NF)	--	509	--	1,500

* Allowable stress level for the magnesium was based on a skin temperature of 435 °F.

TABLE 8

NOMINAL TRAJECTORY DATA FOR THE ARCHER SOUNDING ROCKET

Time	Velocity (ft/sec)	Altitude (ft)	Range (ft)	Flight Path Angle (deg)	Acceleration (g's)	Weight (lbs)
0	238	30	5	80.0	3.32	318.84
10	1362	7770	2010	73.7	3.40	259.32
20	2498	25940	7950	70.6	4.11	199.80
30	4336	57020	19570	68.7	7.87	140.28
35	5861	80510	28710	68.0	11.28	110.52
40	5622	107040	39790	67.4	-1.19	"
50	5296	157200	61300	66.1	- .94	"
60	5004	204080	82760	64.6	- .91	"
70	4720	247800	104190	63.0	- .89	"
80	4442	288410	125600	61.2	- .88	"
90	4170	325900	146990	59.1	- .86	"
100	3905	360300	168370	56.8	- .84	"
110	3647	391620	189710	54.2	- .81	"
120	3399	419860	211030	51.2	- .78	"
130	3163	445030	232310	47.7	- .74	"
140	2940	467140	253560	43.8	- .69	"
150	2733	486200	274770	39.2	- .63	"
160	2547	502210	295930	33.9	- .56	"
170	2386	515170	317050	27.8	- .47	"
180	2254	525100	338120	21.0	- .36	"
190	2158	531990	359140	13.5	- .23	"
200	2103	535850	380110	5.4	- .09	"
210	2090	536670	401010	-3.0	.05	"
220	2122	534460	421860	-11.2	.19	"
230	2196	529220	442630	-19.1	.33	"
240	2308	520940	463340	-26.4	.44	"
250	2453	509620	483980	-32.9	.54	"
260	2626	495260	504550	-38.6	.62	"
270	2821	477850	525030	-43.6	.69	"
280	3036	457390	545440	-47.9	.74	"
290	3266	433870	565760	-51.6	.78	"
300	3508	407290	585990	-54.9	.82	"
310	3761	377630	606140	-57.7	.84	"

TABLE 8

NOMINAL TRAJECTORY DATA FOR THE ARCHER SOUNDING ROCKET

Time	Velocity (ft/sec)	Altitude (ft)	Range (ft)	Flight Path Angle (deg)	Acceleration (g's)	Weight (lbs)
320	4022	344880	626190	-60.2	.87	110.52
330	4291	309040	646140	-62.4	.88	"
340	4566	270100	665990	-64.3	.90	"
350	4847	228030	685740	-66.0	.91	"
360	5131	182850	705380	-67.6	.91	"
370	5411	134560	724900	-69.0	.86	"
380	5607	83460	744170	-70.2	.09	"
390	4848	33120	761920	-71.4	-6.29	"
399.868	2259	0	772730	-73.3	-7.20	"

TABLE 9

WIND AND Q.E. EFFECTS ON THE ARCHER SOUNDING ROCKET

Q.E. (deg)	Wind Velocity (ft/sec)	Wind Direction	Burnout Alt(ft)	Burnout Range (ft)	Max. Alt(ft)	Impact Range (ft)	Impact Cross Range (ft)
87	0		85,300	8,940	622,660	260,740	0
"	20	Tail	85,660	-3,700	629,440	-120,930	0
"	20	Head	82,890	21,110	578,200	601,140	0
"	20	Cross	84,250	8,860	602,350	253,300	369,710
82	0		82,380	23,410	569,520	647,980	0
"	20	Tail	85,040	11,250	618,500	314,680	0
"	20	Head	77,960	34,400	492,570	883,020	0
"	20	Cross	81,370	23,200	550,800	629,280	345,150
80	0		80,510	28,910	536,670	772,720	0
"	20	Tail	84,040	17,160	600,220	478,090	0
"	20	Head	75,420	39,280	450,970	953,440	0
"	20	Cross	79,520	28,660	519,000	750,220	329,630
78	0		78,370	34,200	498,710	874,420	0
"	20	Tail	82,600	22,960	574,490	627,480	0
"	20	Head	72,600	43,860	406,840	996,940	0
"	20	Cross	77,320	33,900	482,030	848,670	311,240
73	0		71,290	46,210	388,060	1,010,800	0
"	20	Tail	77,250	36,650	482,850	909,650	0
"	20	Head	64,550	53,900	293,330	984,990	0
"	20	Cross	70,420	45,820	374,870	979,660	254,880

TABLE 10

WIND WEIGHTING FACTORS FOR THE ARCHER SOUNDING ROCKET

Layer (ft x 10^{-3})	Wind Weighting Factors (Range and Cross Wind)
0-0.5	-.557
0.5-1.0	-.135
1.0-1.5	-.067
1.5-2.0	-.041
2.0-3.0	-.049
3.0-4.0	-.028
4.0-6.0	-.031
6.0-8.0	-.018
8.0-10	-.012
10-12	-.008
12-15	-.009
15-19	-.009
19-24	-.008
24-29	-.006
29-34	-.004
34-44	-.006
44-54	-.004
54-64	-.003
64-84	-.004
84-104	0

Unit wind effect for tail wind = -14,700 ft. per ft/sec
Unit wind effect for head wind = - 9,000 ft. per ft/sec
Unit wind effect for lateral wind = -16,500 ft. per ft/sec.
Q.E. correction for range wind = -.237 degrees per ft/sec.
Azimuth correction for cross wind = 1.19 degrees per ft/sec.

TABLE 11

DISPERSION DATA FOR THE ARCHER SOUNDING ROCKET

Cause of Dispersion	Variation	Range Deflection(ft)	Cross-range Deflection(ft)
Weight Variation	$2\sigma = \pm 4\%$	$\mp$64,000(est)	
	$3\sigma = \pm 6\%$	$\mp$96,000(est)	
Thrust Variation	$2\sigma = \pm 10\%$	$\pm$180,000(est)	
	$3\sigma = \pm 15\%$	$\pm$255,000	
Errors in Drag Estimates	$2\sigma = \pm 20\%$	$\mp$78,000(est)	
	$3\sigma = \pm 30\%$	$\mp$116,000	
Error in Wind Velocity	$2\sigma = \pm 6$ ft/sec	$\mp$84,000	$\mp$99,000
	$3\sigma = \pm 9$ ft/sec	$\mp$126,000	$\mp$148,000
Launch Errors and Malalignment	$2\sigma = \pm 1°$	$\mp$57,000	$\pm$14,000
	$3\sigma = \pm 1.5°$	$\mp$86,000	$\pm$21,000
TOTAL DISPERSION	2σ	230,000	100,000
	3σ	333,000	149,000

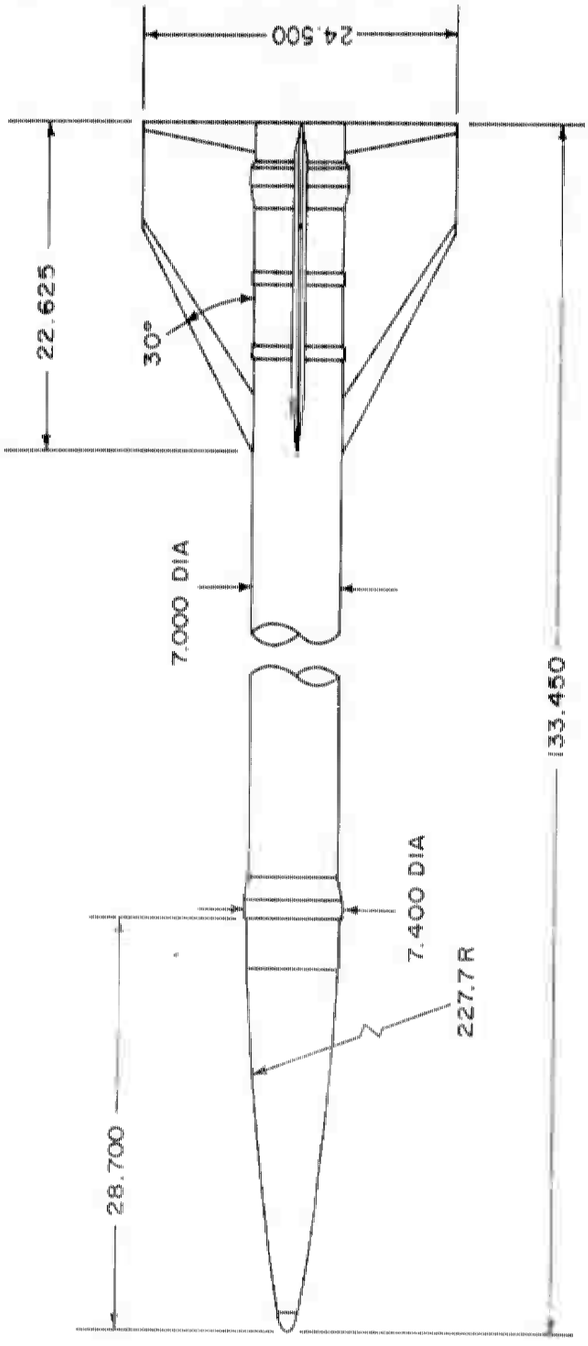

NOTE:
DIMENSIONS ARE IN INCHES

FIG. 1 ARCHER ASSEMBLY DRAWING

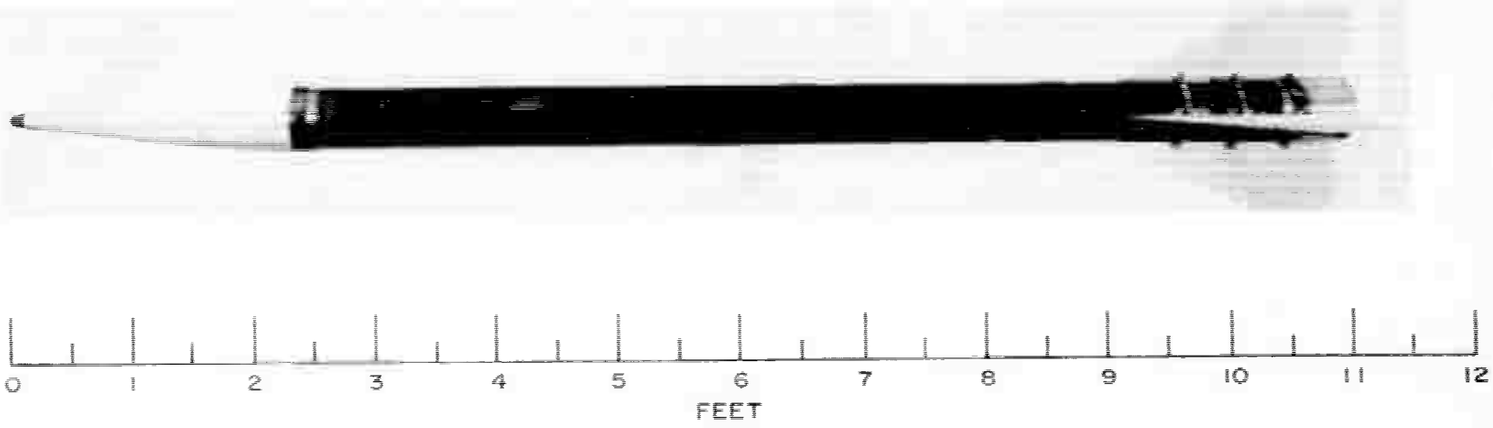

NOLTR 63-144

FIG. 1-A ARCHER TEST VEHICLE PHOTOGRAPH

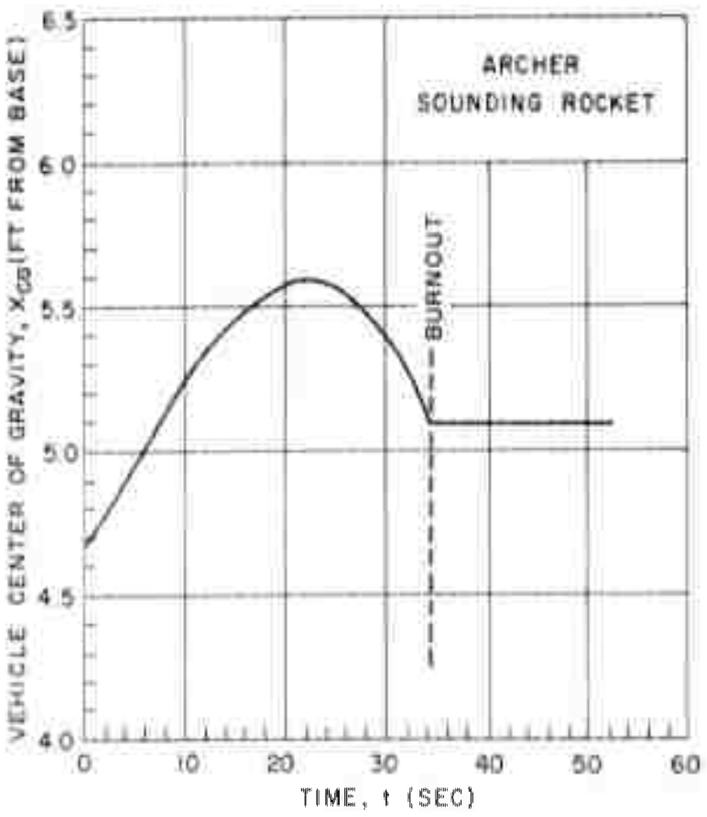

FIG. 2 VEHICLE CENTER OF GRAVITY AS A FUNCTION OF TIME

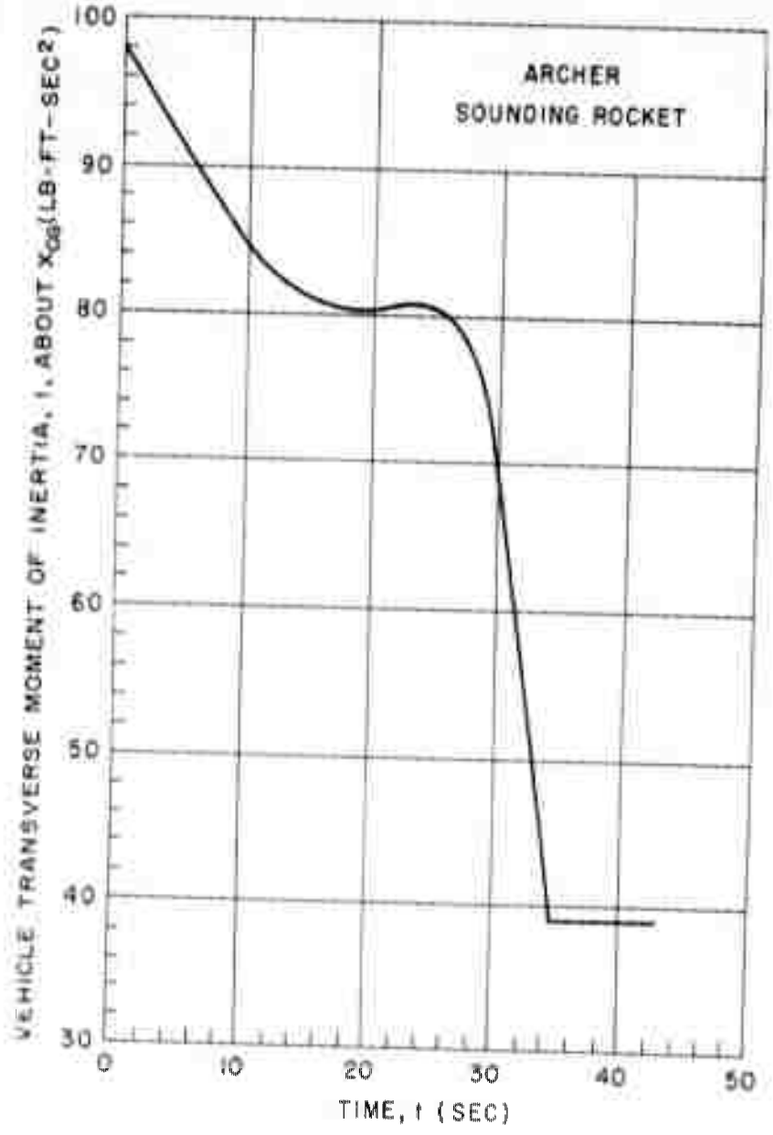

FIG. 3 VEHICLE TRANSVERSE MOMENT OF INERTIA AS A FUNCTION OF TIME

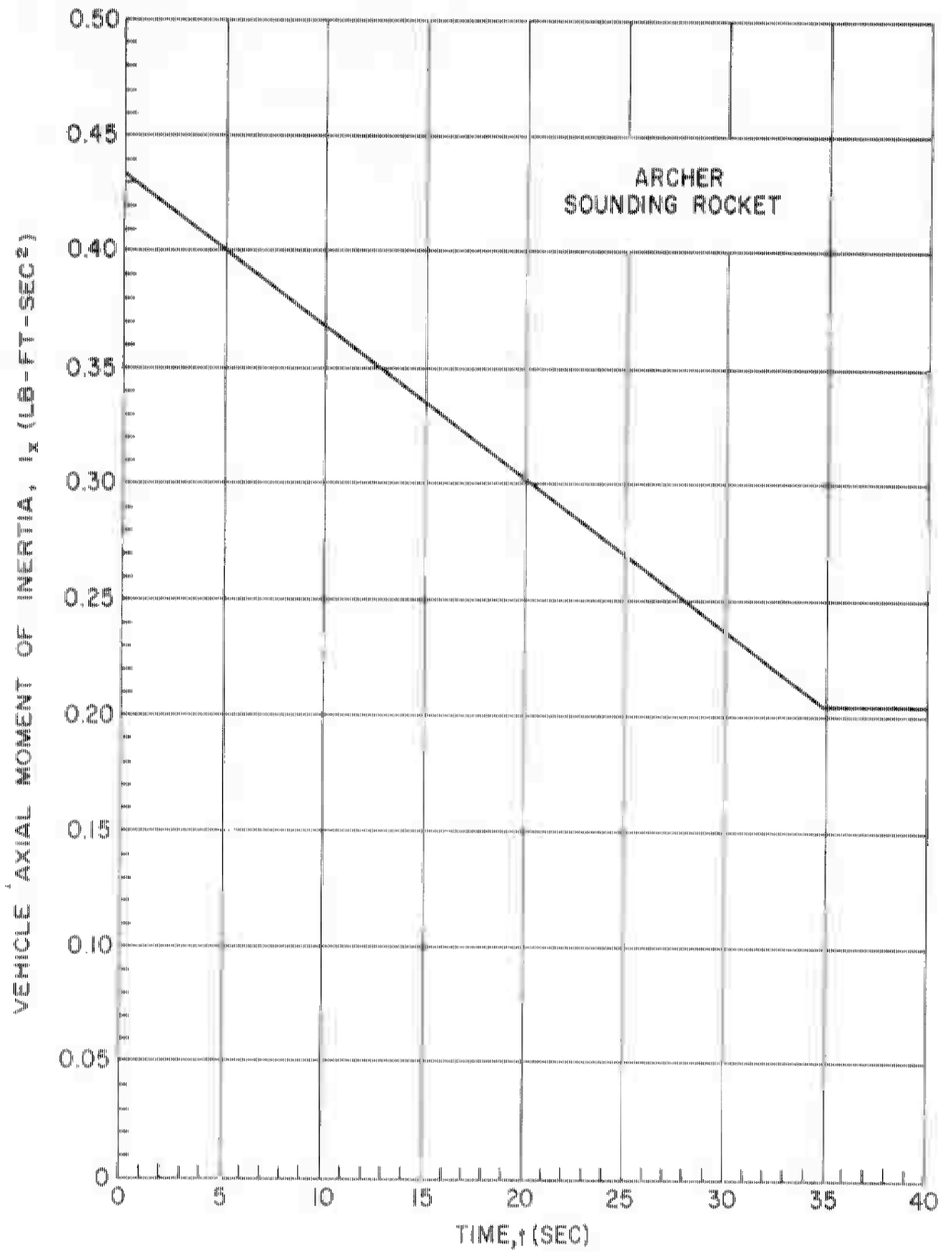

FIG. 4 VEHICLE AXIAL MOMENT OF INERTIA AS A FUNCTION OF TIME

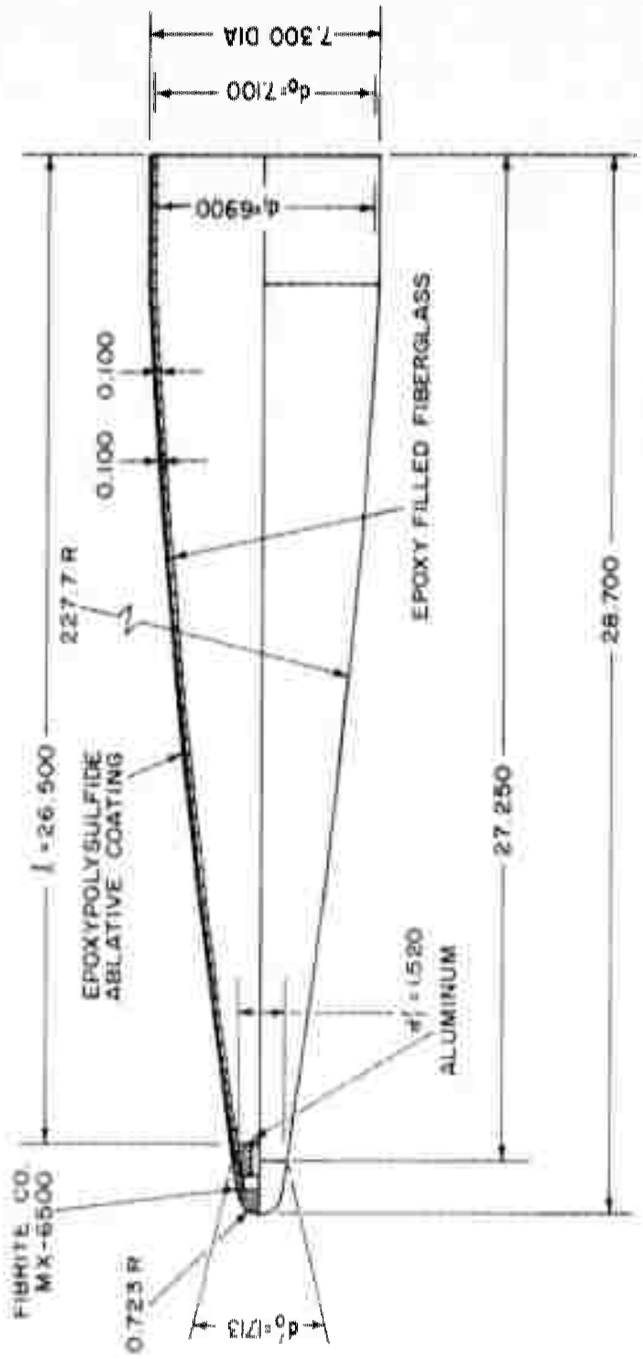

FIG. 5 ARCHER NOSE-CONE DRAWING

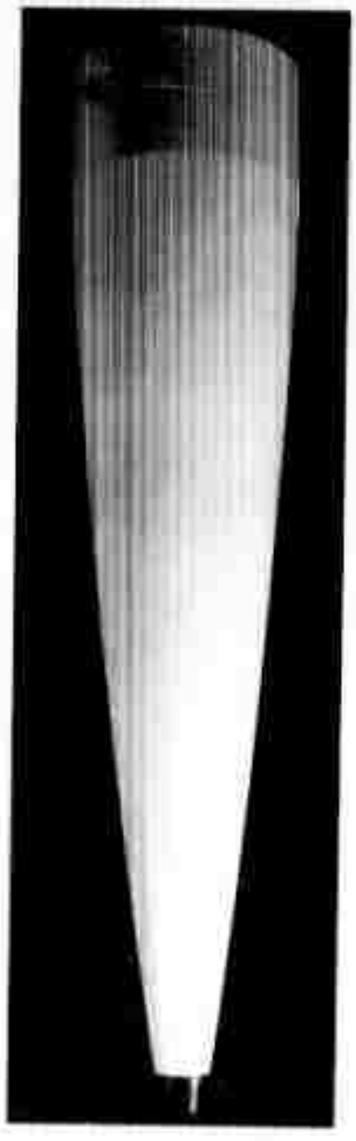

FIG. 5 - A ARCHER NOSE-CONE PHOTOGRAPH

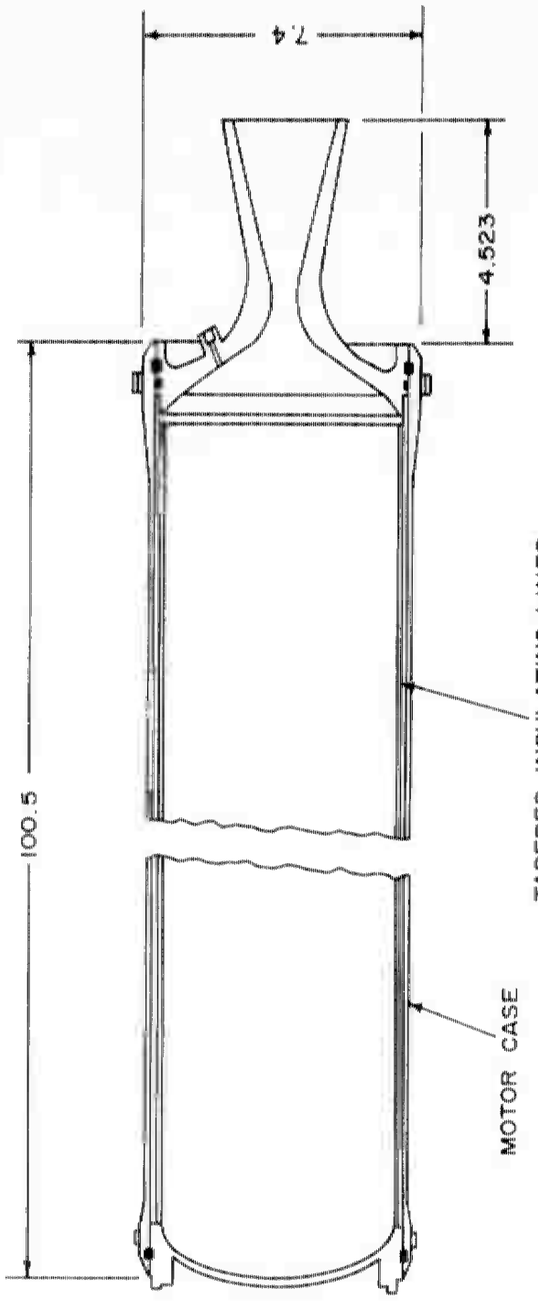

NOTE:
DIMENSIONS ARE IN INCHES

FIG. 6 ARCHER ENGINE CONFIGURATION

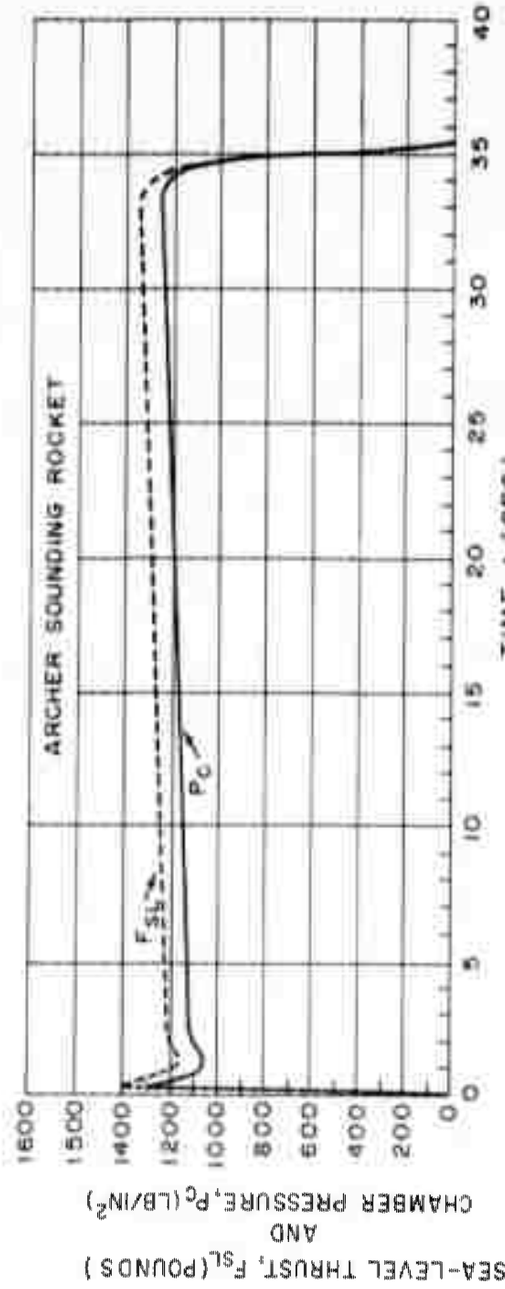

FIG 7 THRUST AND CHAMBER PRESSURE AS A FUNCTION OF TIME

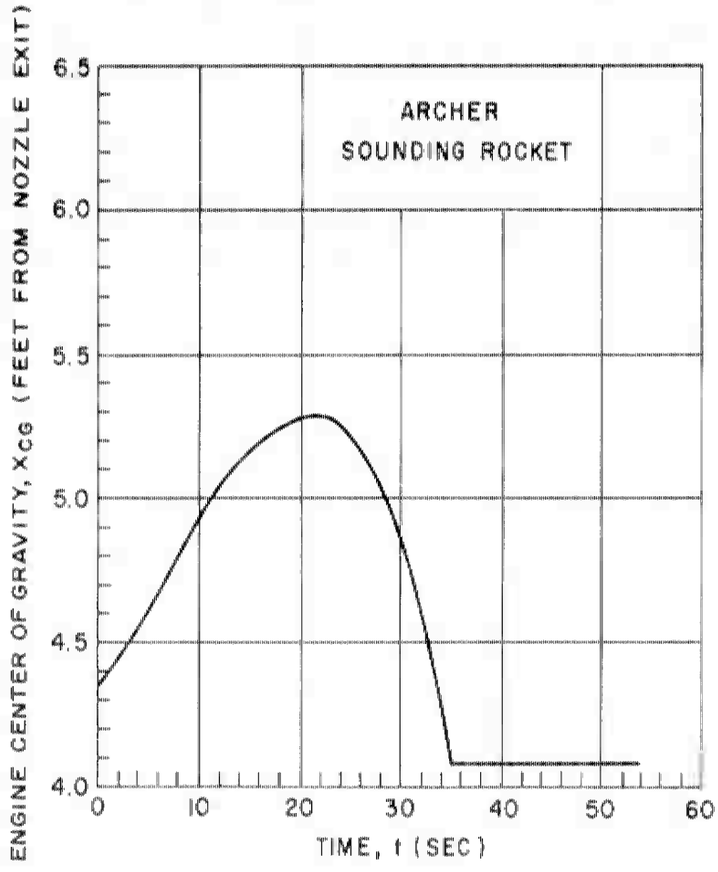

FIG. 8 ENGINE CENTER OF GRAVITY AS A FUNCTION OF TIME

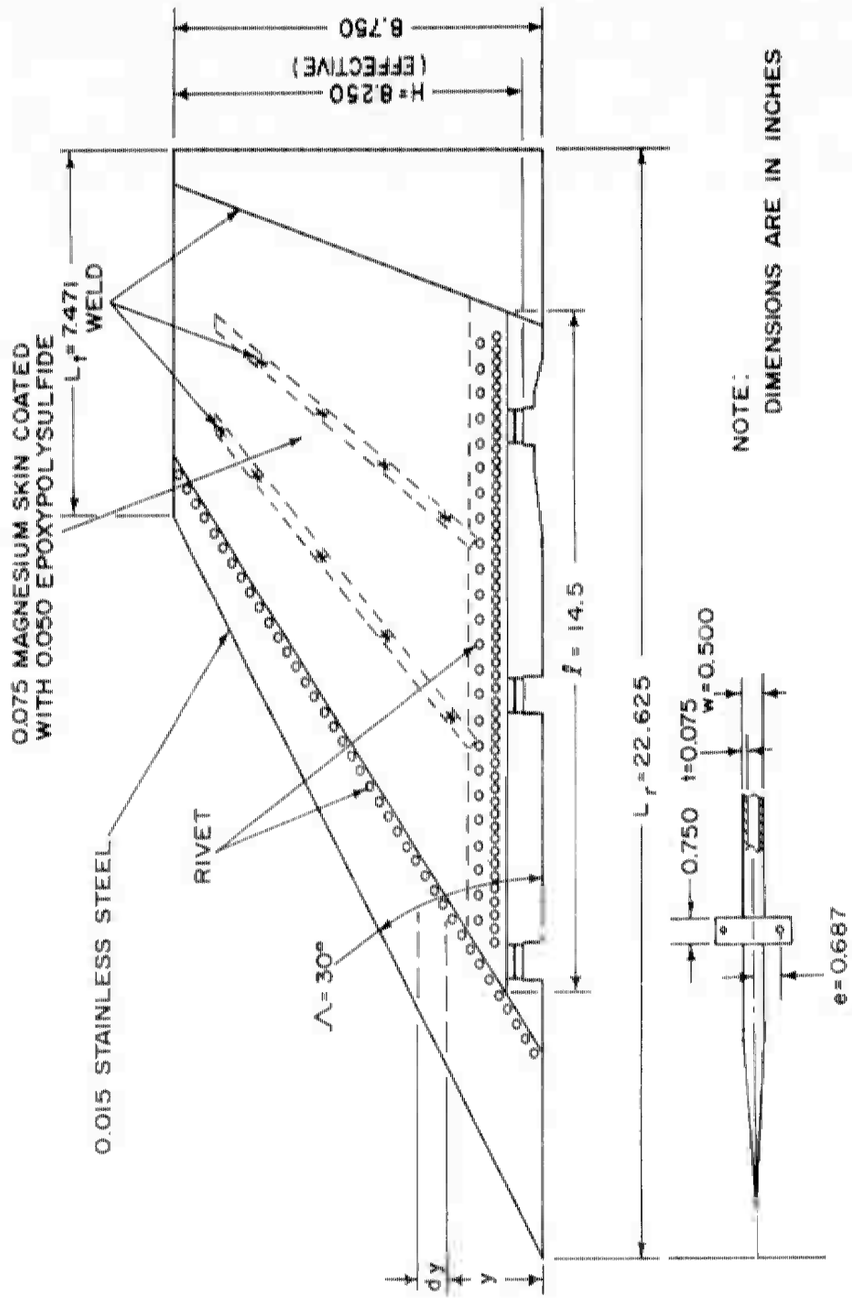

FIG. 9 ARCHER FIN DRAWING

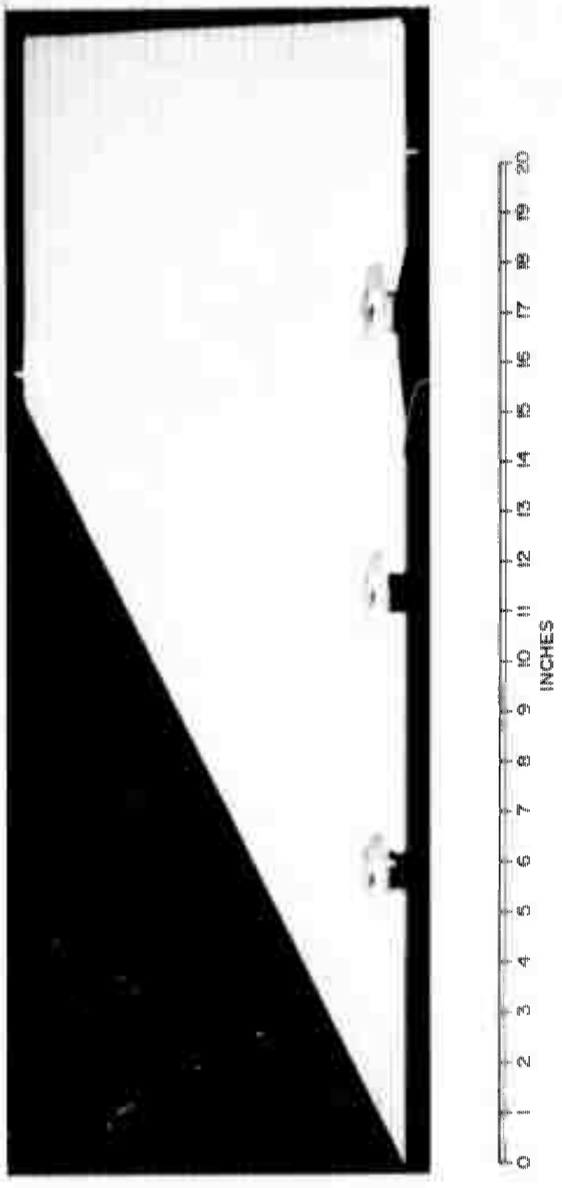

FIG. 9 -A ARCHER FIN PHOTOGRAPH

FIG. 10 ARCHER WIND-TUNNEL MODEL

α = 0°

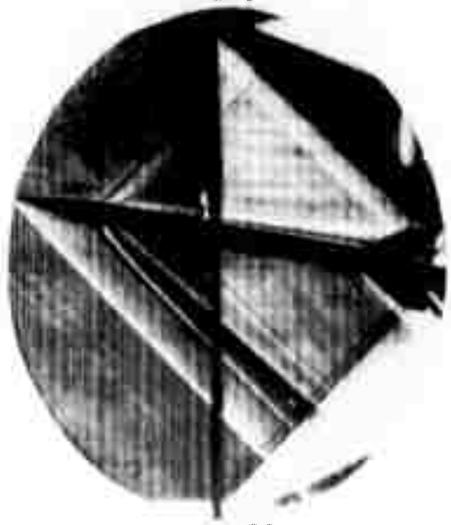

α = 10°

FIG. 11 ARCHER SCHLIEREN PHOTOGRAPHS AT MACH NUMBER 1.52

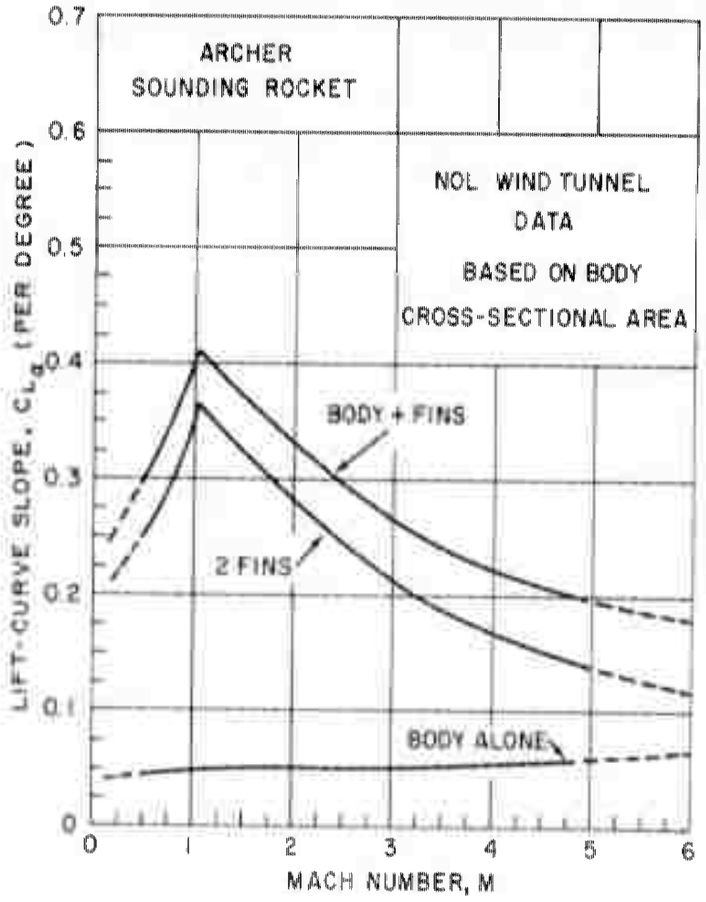

FIG. 12 LIFT-CURVE SLOPES AS A FUNCTION OF MACH NUMBER

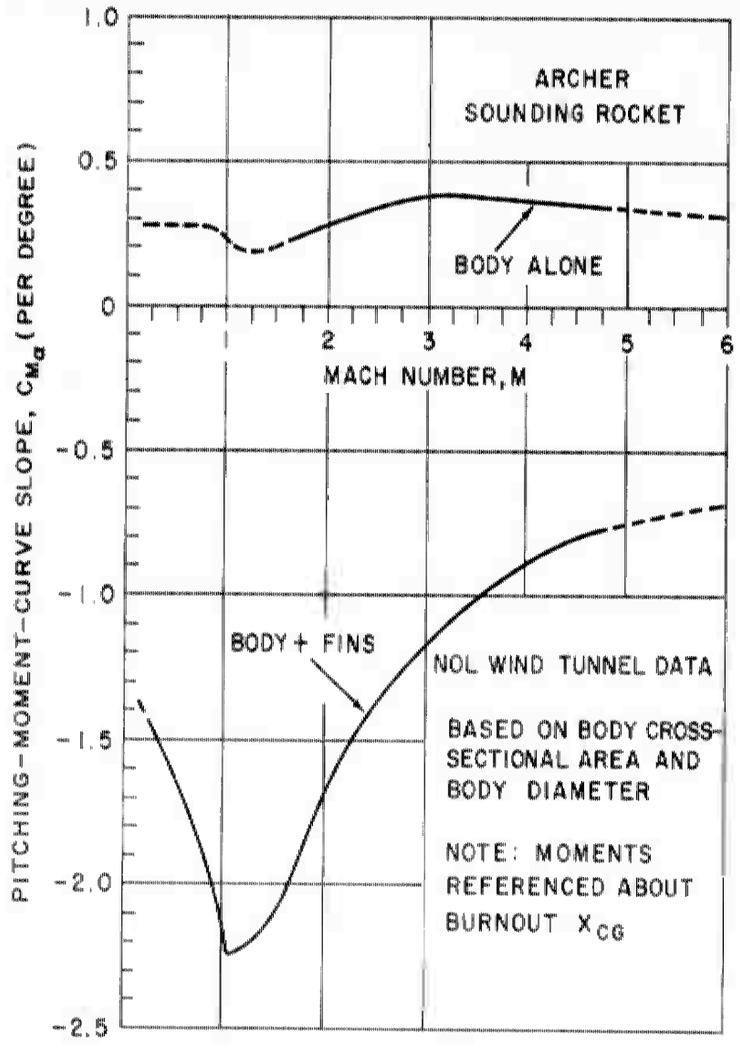

FIG. 13 PITCHING-MOMENT-CURVE SLOPES AS A FUNCTION OF MACH NUMBER

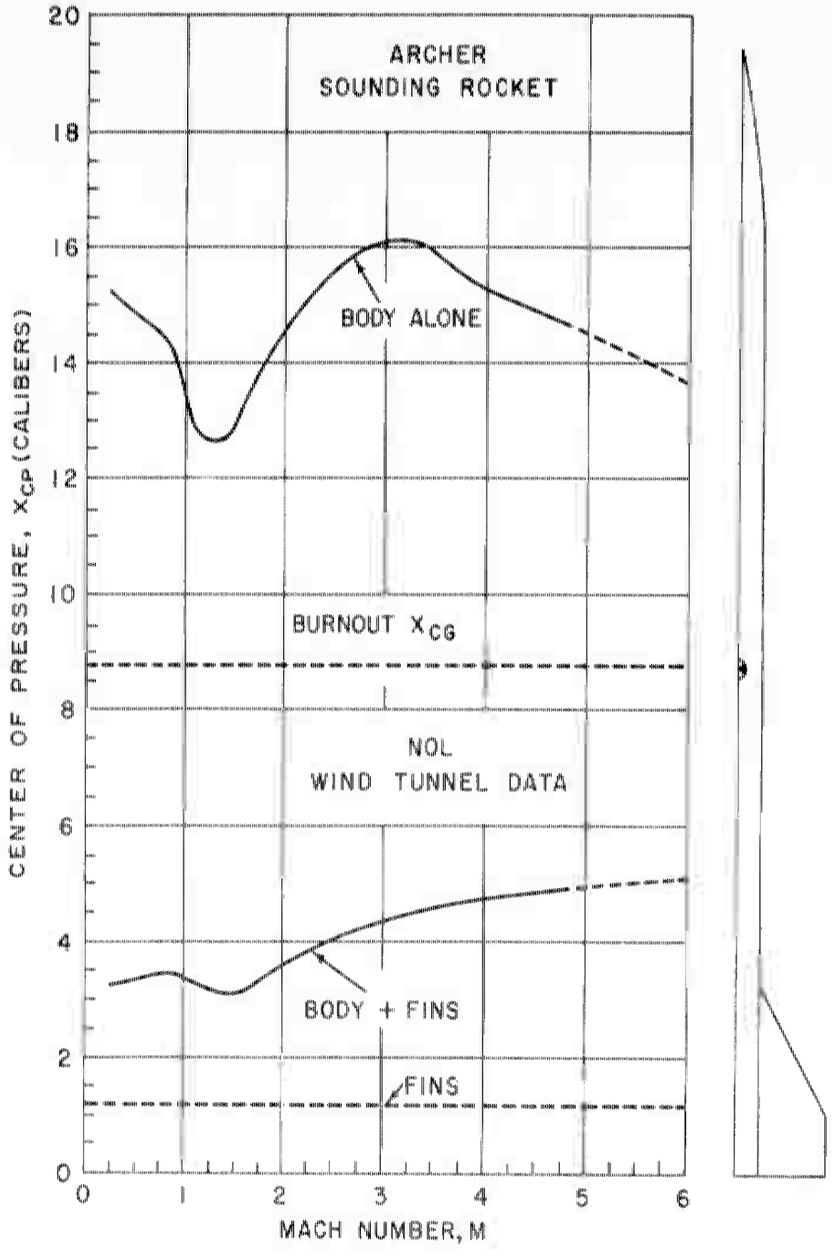

FIG. 14 CENTER OF PRESSURES AS A FUNCTION OF MACH NUMBER

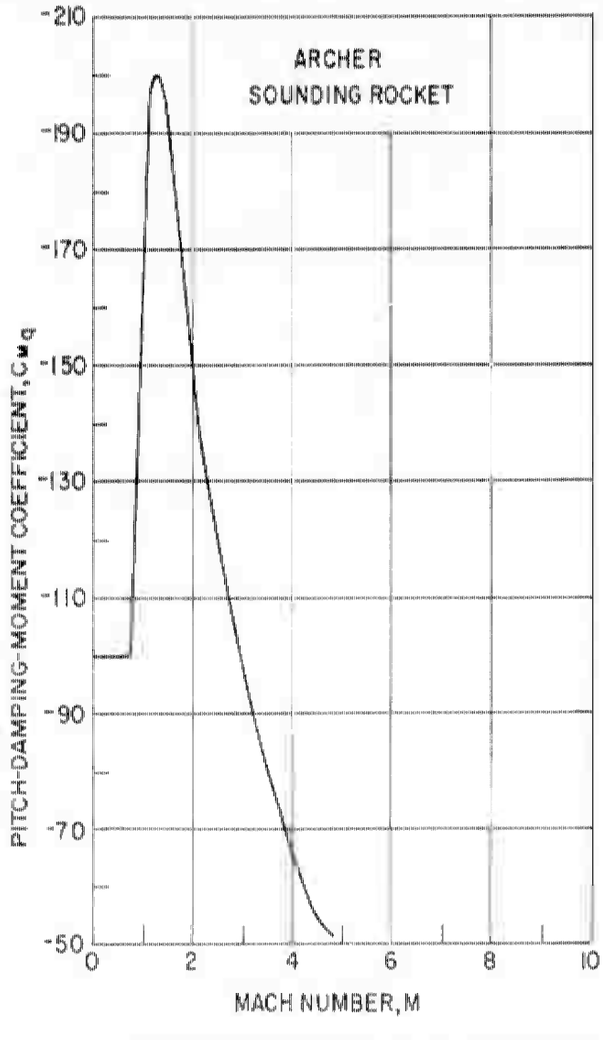

FIG. 15 PITCH-DAMPING-MOMENT COEFFICIENT AS A FUNCTION OF MACH NUMBER

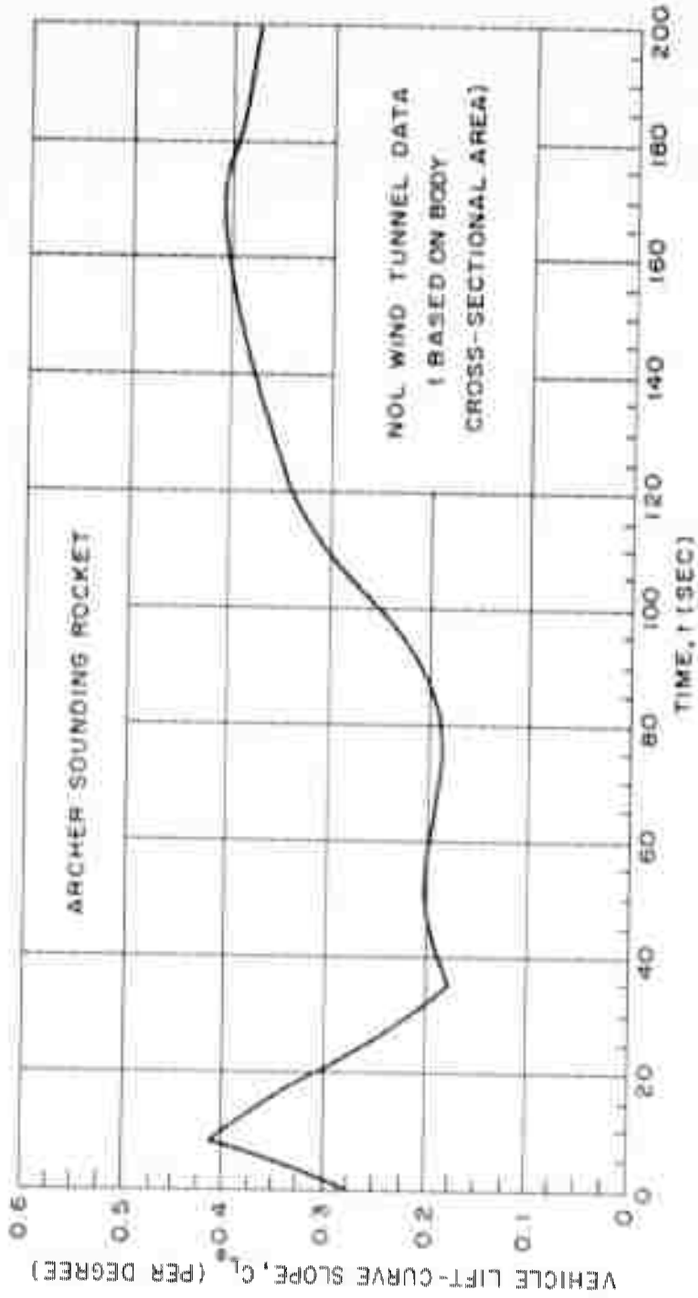

FIG. 16 VEHICLE LIFT-CURVE SLOPE AS A FUNCTION OF TIME

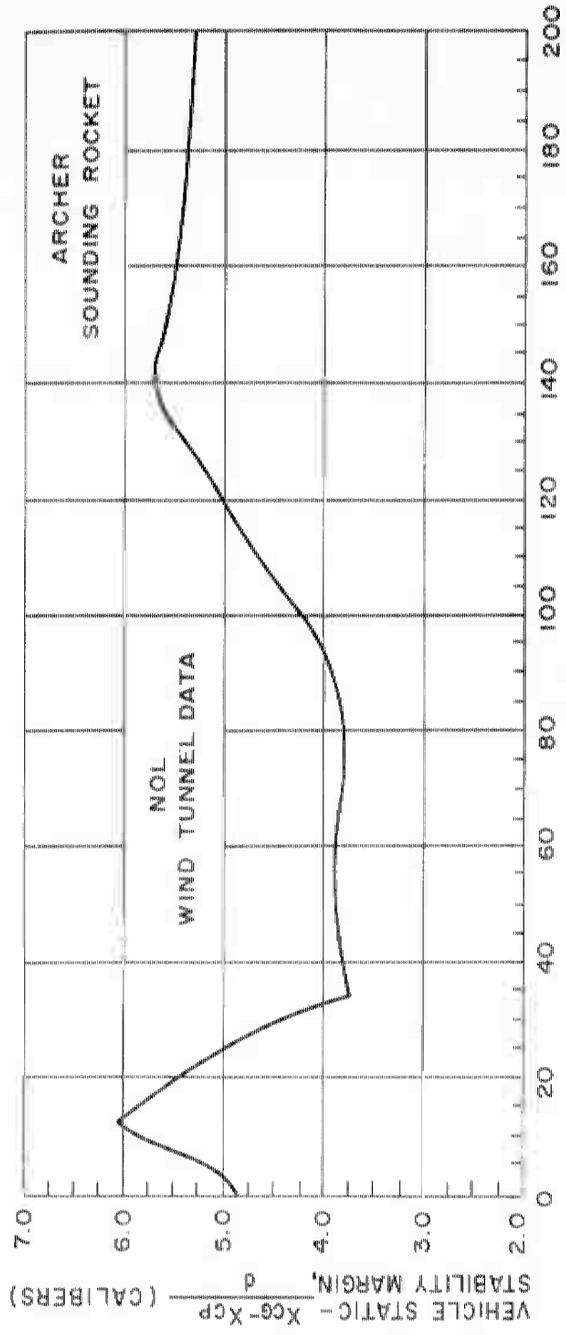

FIG. 17 VEHICLE STATIC - STABILITY MARGIN AS A FUNCTION OF TIME

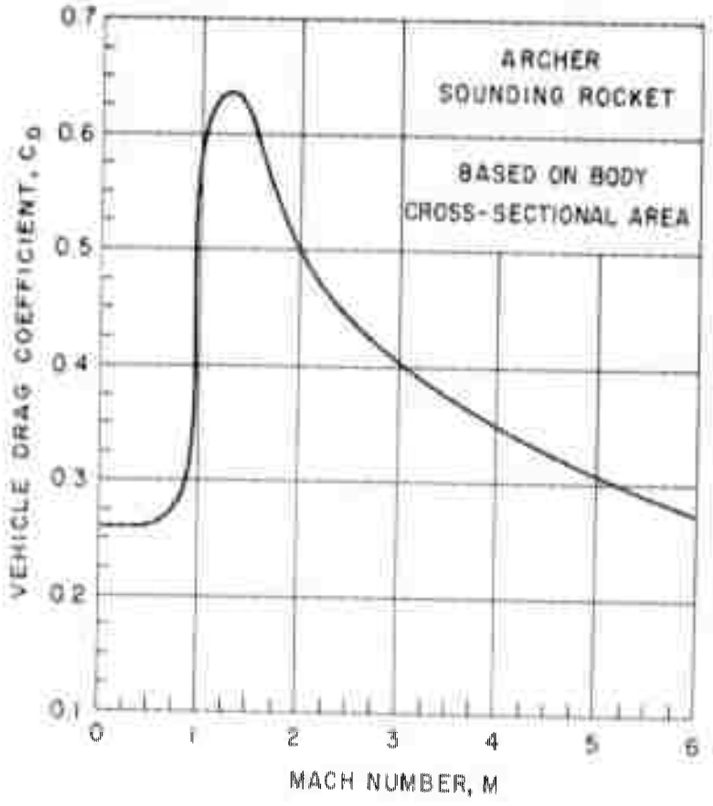

FIG. 18 VEHICLE DRAG COEFFICIENT AS A FUNCTION OF MACH NUMBER

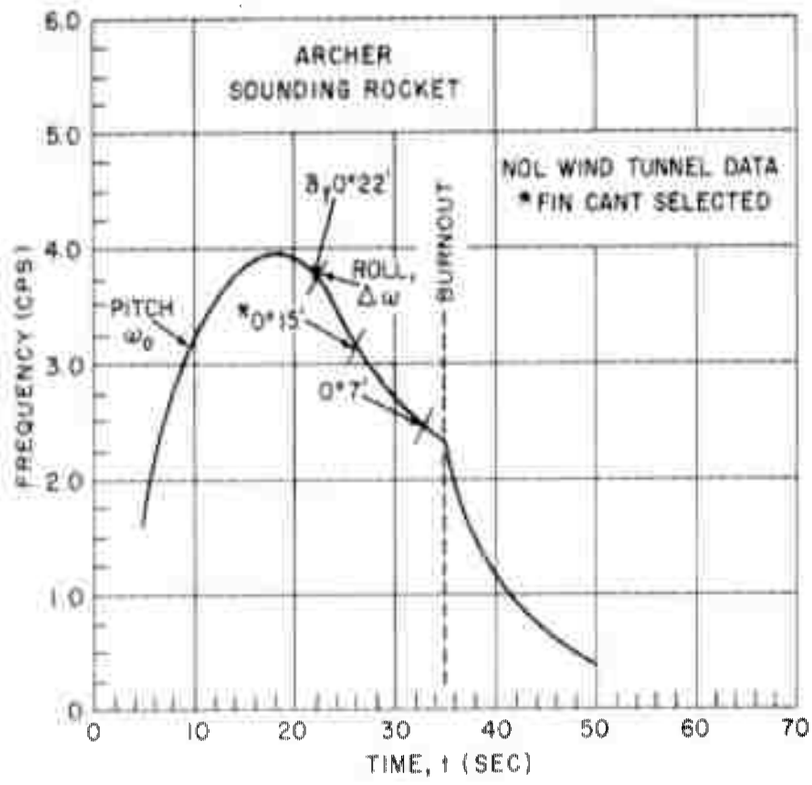

FIG. 19 NATURAL FREQUENCIES AS A FUNCTION OF TIME

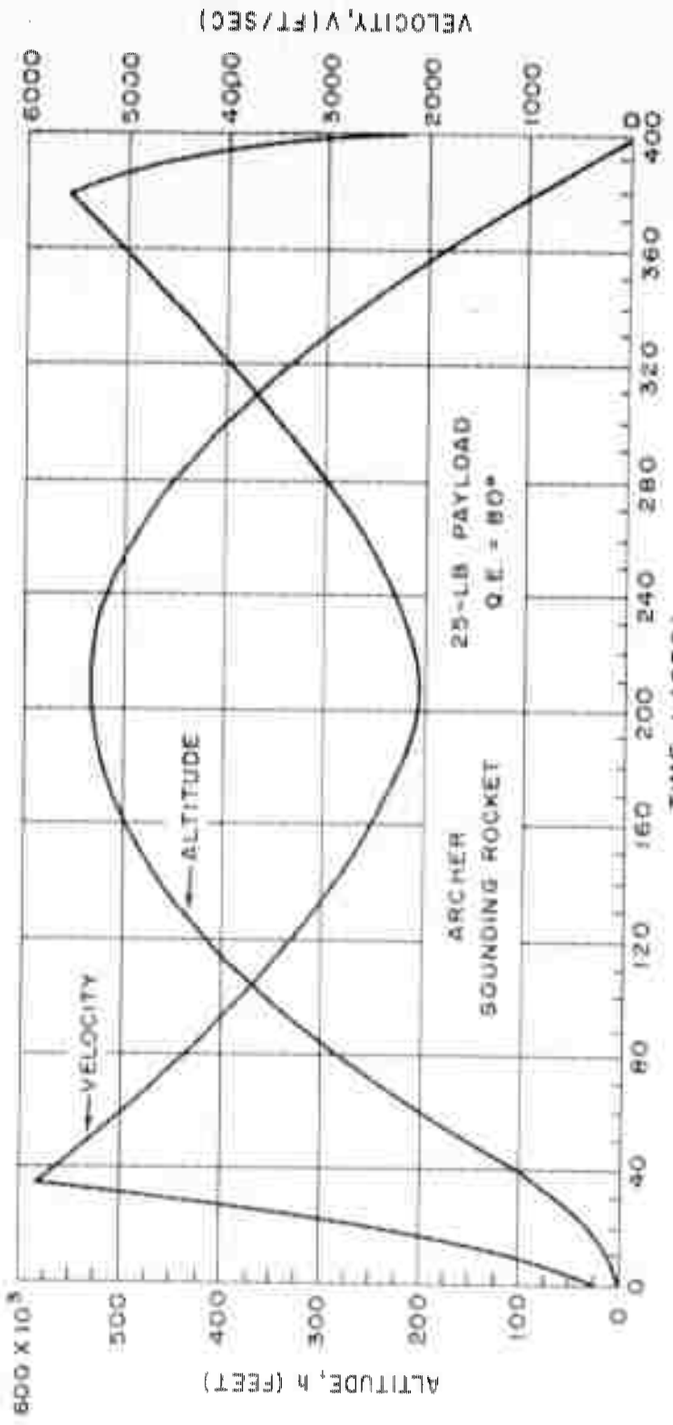

FIG. 20 ALTITUDE AND VELOCITY AS A FUNCTION OF TIME

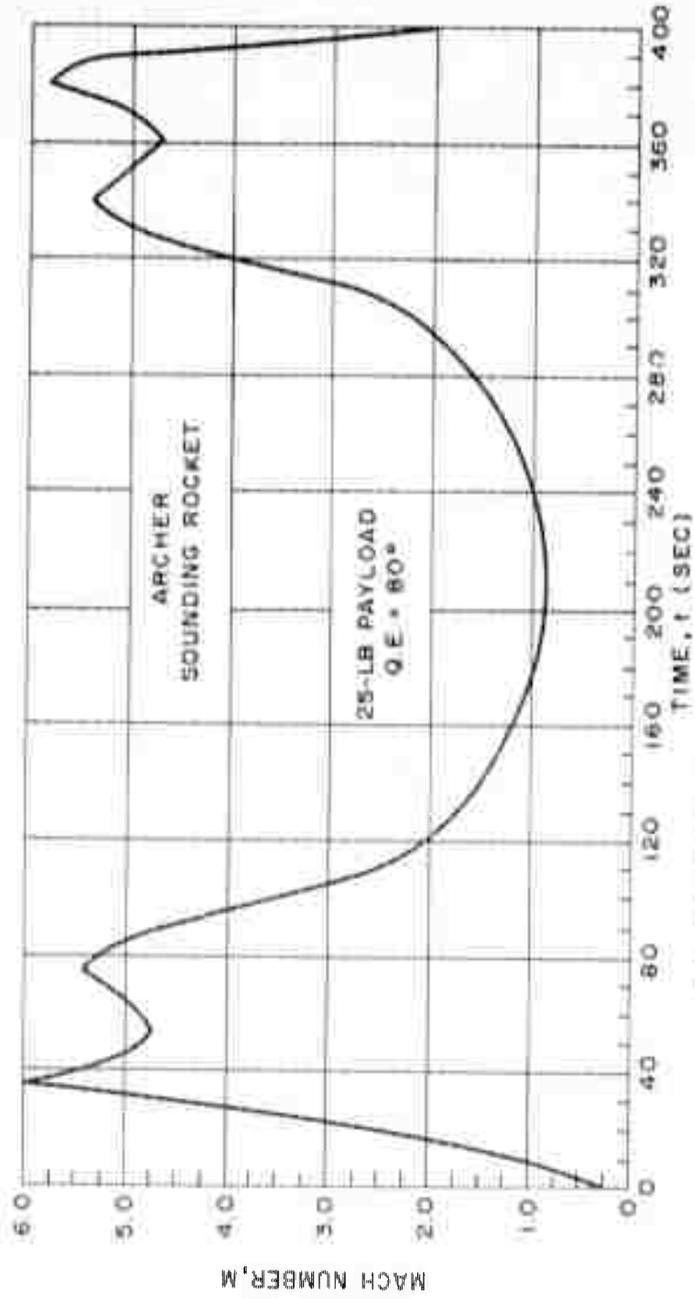

FIG. 21 MACH NUMBER AS A FUNCTION OF TIME

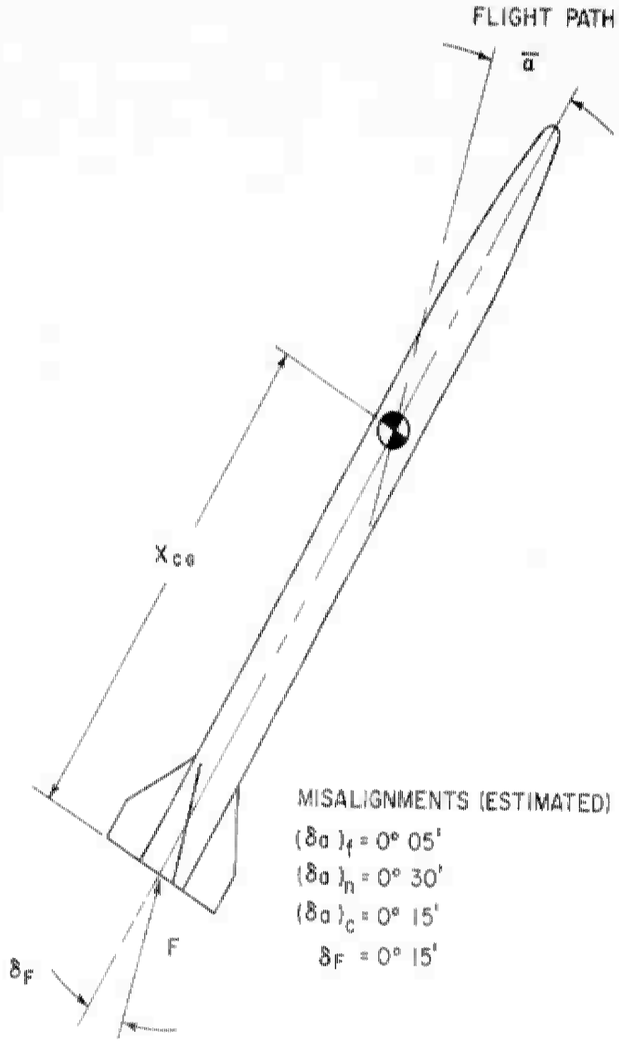

FIG. 22 SIGN CONVENTION

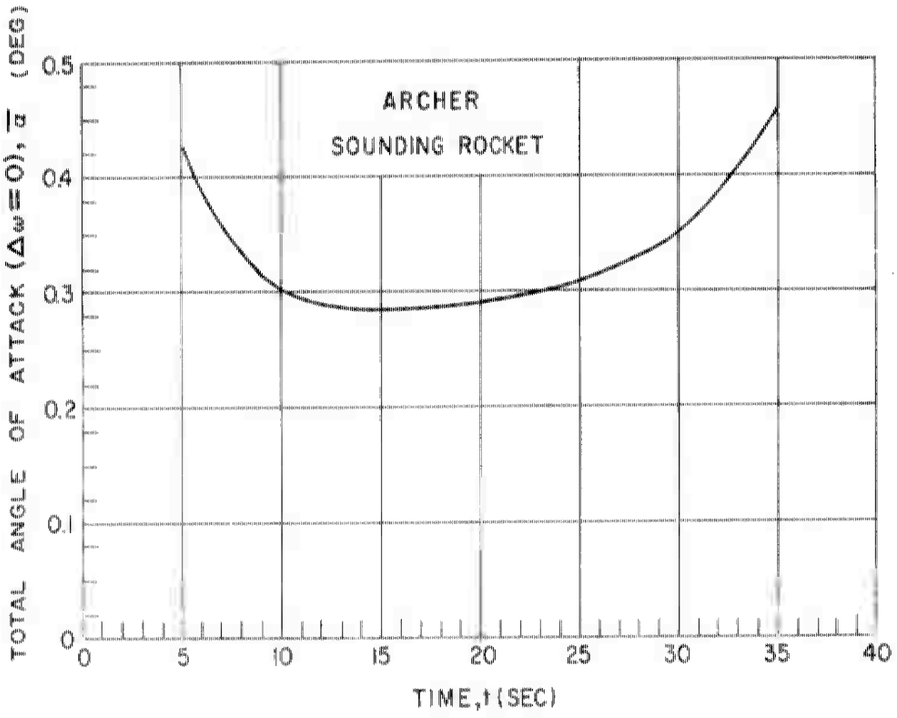

FIG. 23 TOTAL ANGLE OF ATTACK ($\Delta\omega=0$) AS A FUNCTION OF TIME

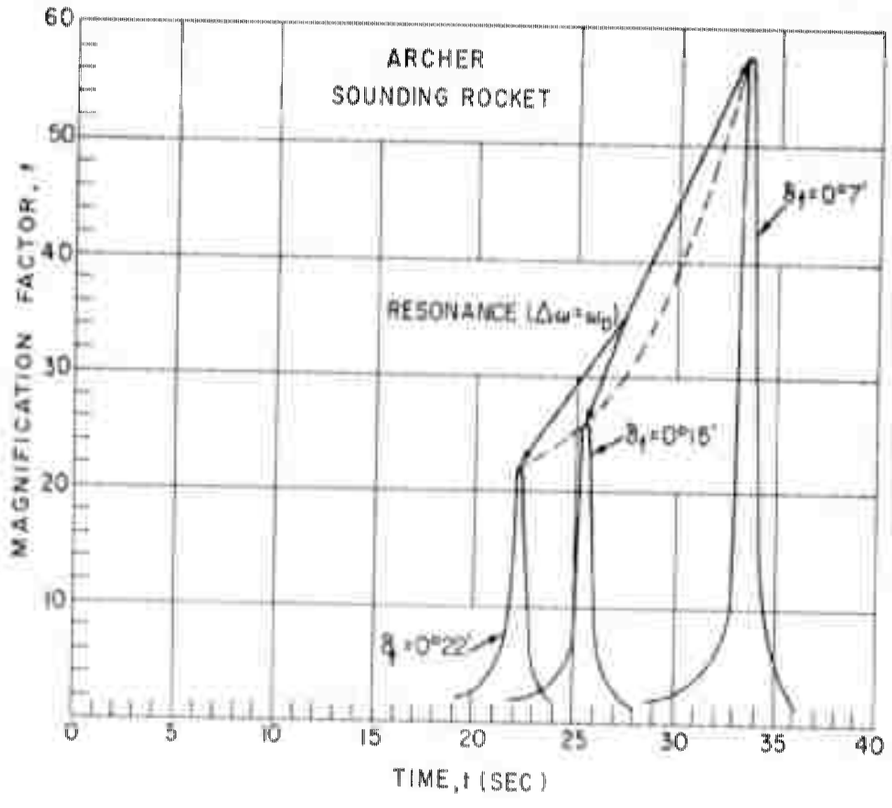

FIG. 24 MAGNIFICATION FACTOR AS A FUNCTION OF TIME

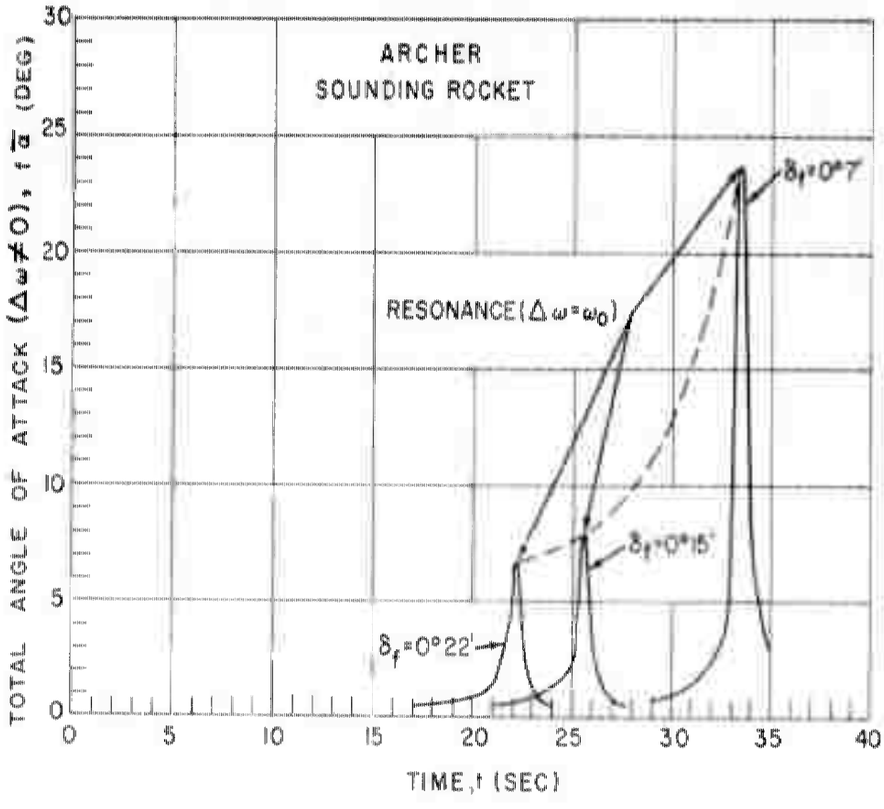

FIG. 25 TOTAL ANGLE OF ATTACK ($\Delta\omega\neq0$) AS A FUNCTION OF TIME

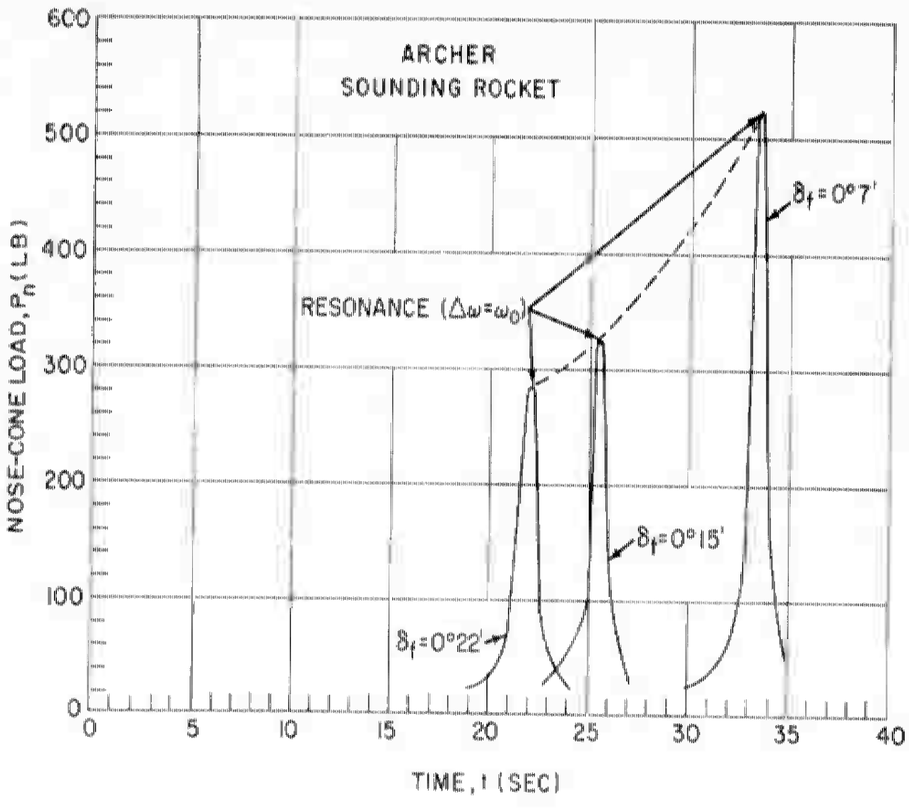

FIG. 26 NOSE-CONE LOADS AS A FUNCTION OF TIME

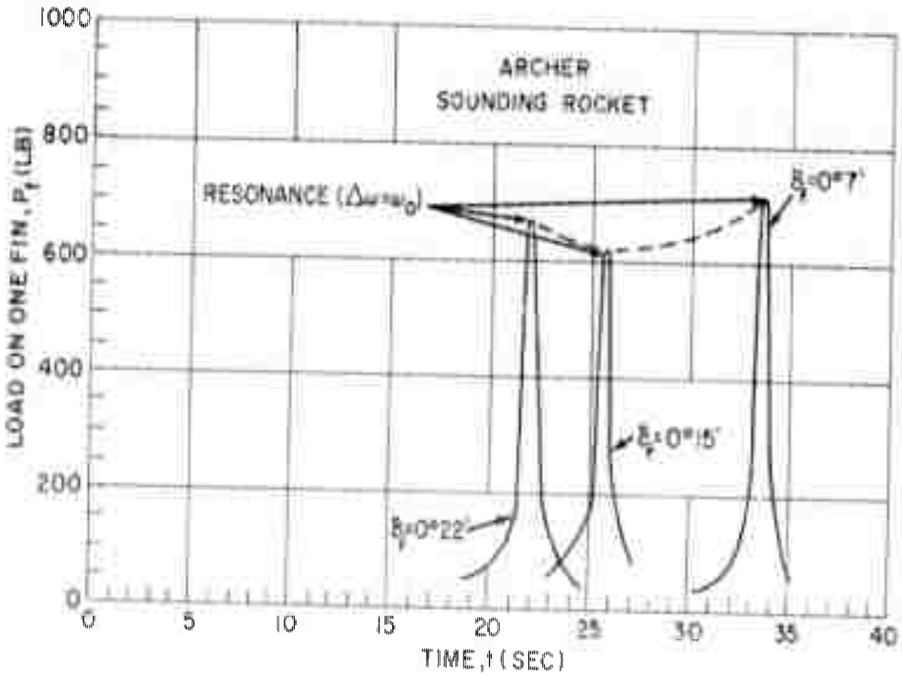

FIG. 27 FIN LOADS AS A FUNCTION OF TIME

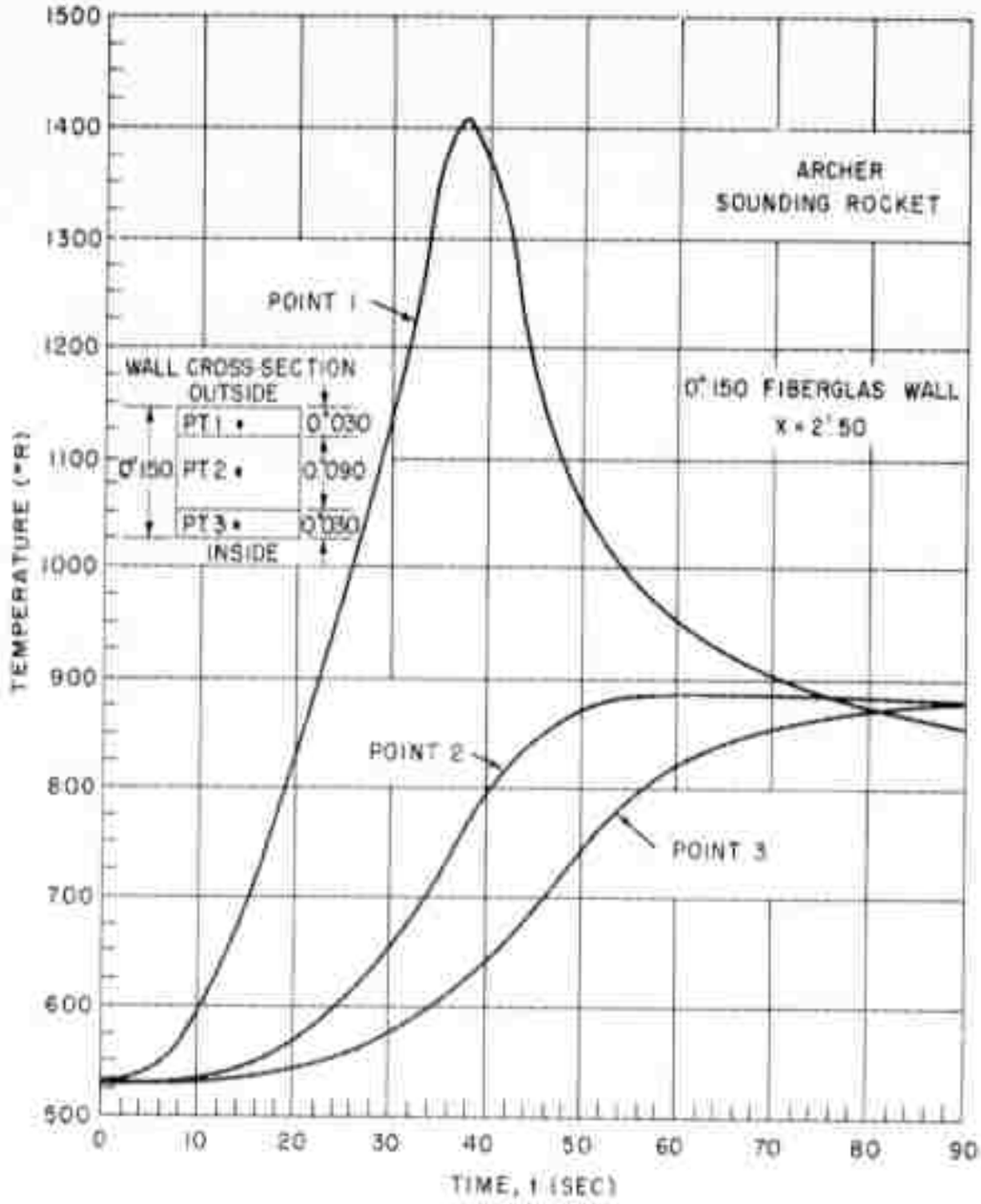

FIG. 28 TEMPERATURE DISTRIBUTION THROUGH NOSE-CONE WALL AS A FUNCTION OF TIME

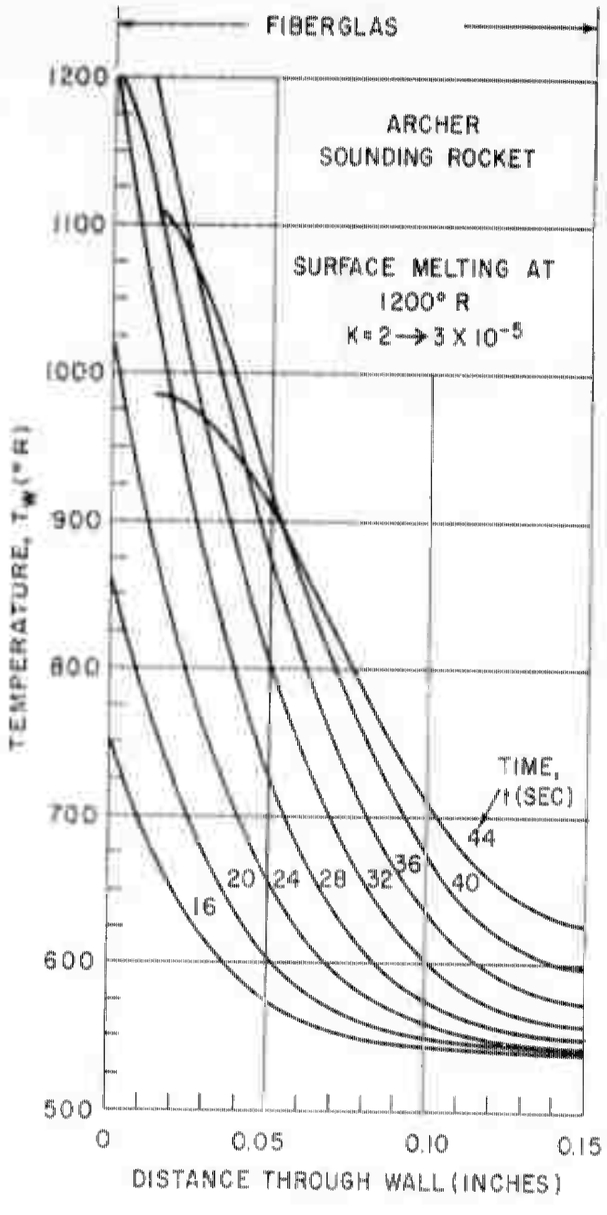

FIG. 29 THERMAL RESPONSE OF NOSE CONE

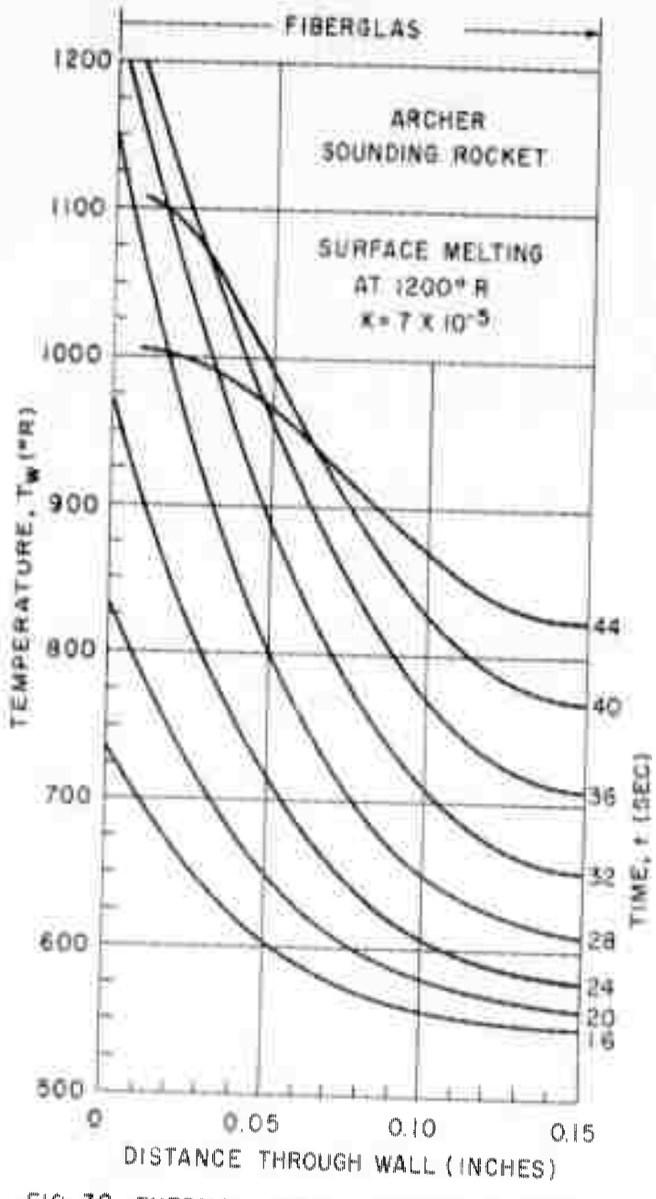

FIG. 30 THERMAL RESPONSE OF NOSE CONE

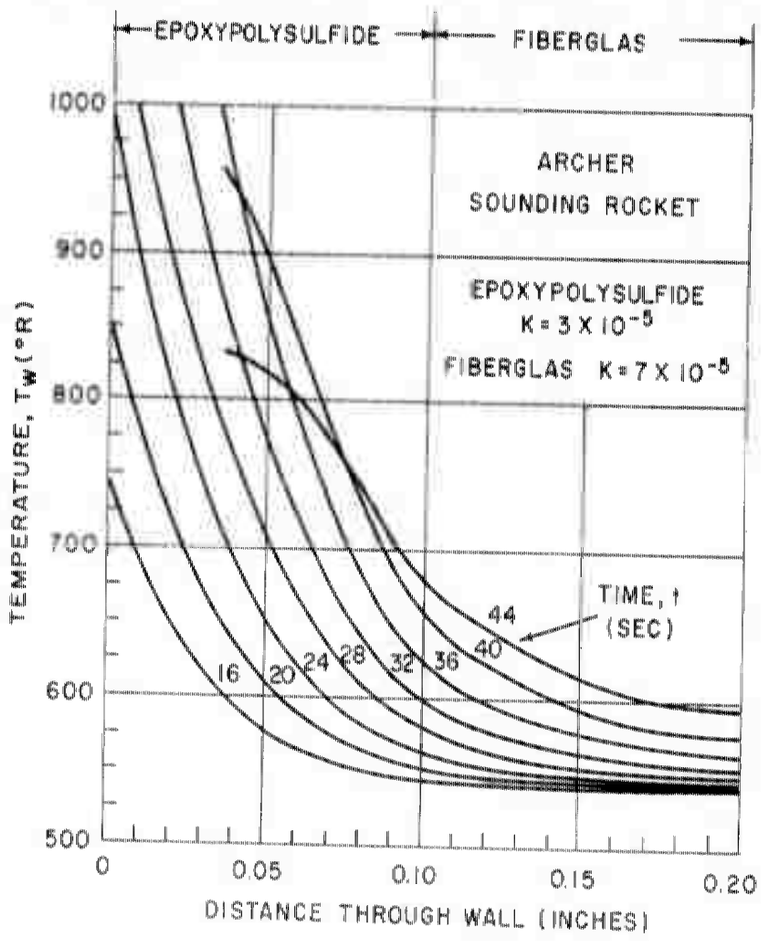

FIG. 31 THERMAL RESPONSE OF NOSE CONE

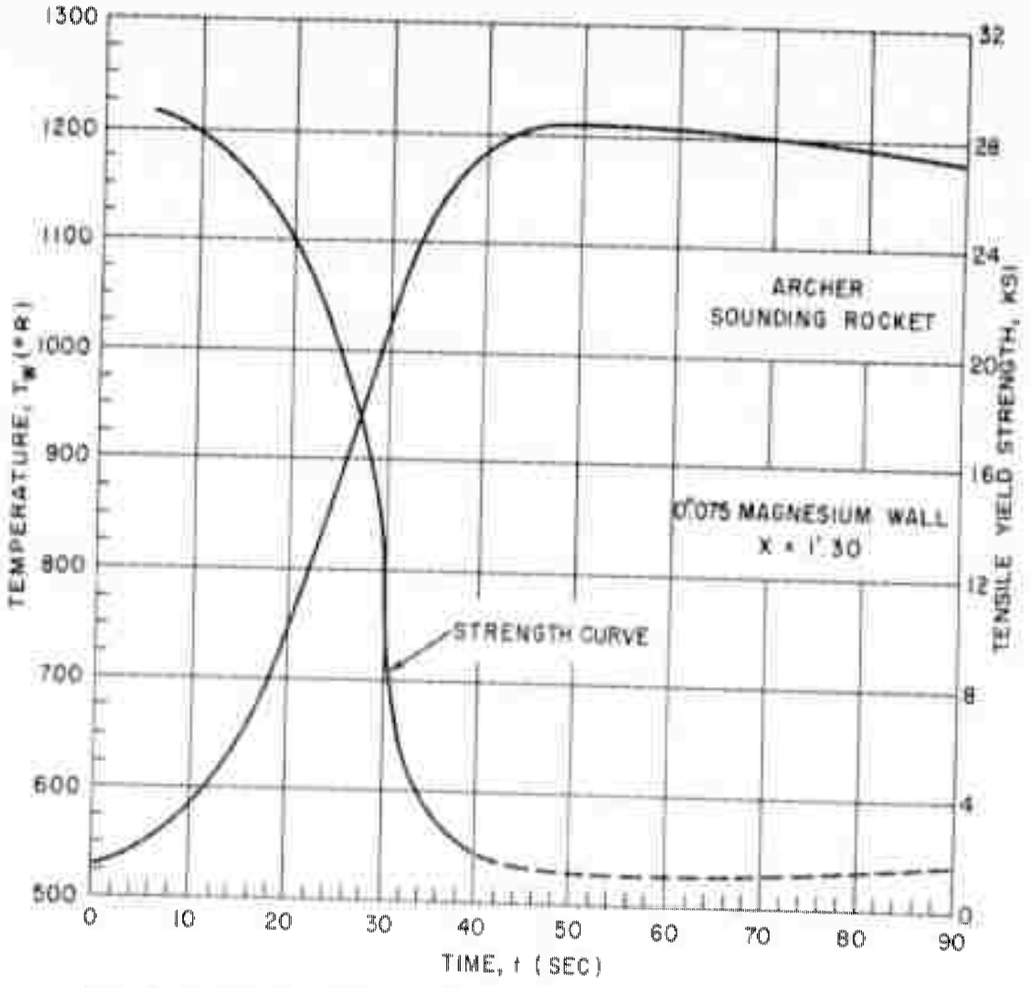

FIG. 32 FIN TEMPERATURE AND YIELD STRENGTH AS A FUNCTION OF TIME

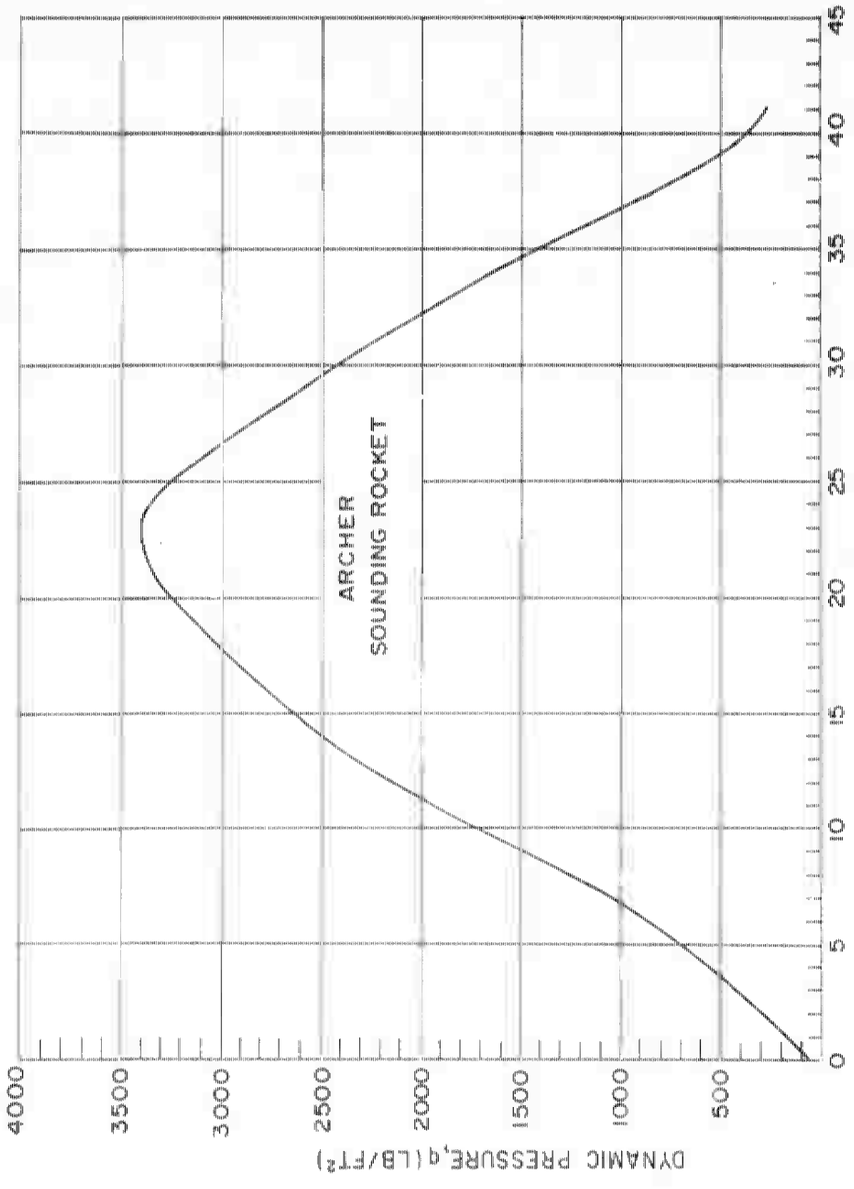

FIG. 33 DYNAMIC PRESSURE AS A FUNCTION OF TIME

APPENDIX A

FLIGHT RESULTS

Prior to the publication of the preceding report, two of the three Archer test vehicles were launched. It was, therefore, considered appropriate to add the results of these tests as well as the recommendations for the third flight to the present publication in the form of an Appendix. These test firings occurred on 16 August and 3 October 1962 at the Pacific Missile Range, Pt. Mugu, California. The first vehicle reached an altitude of approximately 75 miles while the second vehicle reached an altitude of approximately 50 miles. A summary of the free-flight as well as predicted performance of the Archer Rocket is presented in Figures A-1 and A-2.

Analyses of the free-flight data obtained on the two Archer test flights indicate approximately the same pattern of anomalous flight behavior. The chief difference between the two flights was that the first vehicle passed through resonance while the second vehicle locked in resonance. Consequently, the possibility of pitch-roll resonance is considered marginal for the present design and subsequent flights would, probably, result in a random type performance, i.e., a number of vehicles would pass through resonance while the rest would not. It has been the purpose of the NOL, therefore, to examine in detail the possible sources of difficulty contributing to this phenomenon and to recommend corrective measures.

Examination of the engine performance, while not directly discernible from the telemetry data on the first flight, indicates that both flights maintained consistent chamber pressure, approximately 1200 psia, over the expected burning time. Both, however, experienced a delayed ignition of the sustainer of about one second which positions the vehicle free of the launcher prior to ignition and would make it rather sensitive to cross winds. Although the combined amount of thrust and aerodynamic misalignment is difficult to ascertain, it is recognized that an excessive amount would certainly contribute to the resonance problem.

The first vehicle assumed a coning angle of about seven degrees in the region of resonance, from which it recovered. The time and frequency of resonance pass through was approximately 27 seconds and 3 cycles per second, respectively. This performance follows closely that which was predicted. The roll rate increased with velocity up to 5 cycles per second at burnout after which it diminished.

The second vehicle assumed divergent coning angles in the region of resonance from which it did not recover. The time

and frequency of resonance was determined to be approximately 28.5 seconds and 3.40 cycles per second, respectively. Since it was not possible to obtain the pitching frequency directly from the second flight records, it has been calculated based on the free-flight data. This calculated pitching frequency was then superimposed on the rolling frequency obtained from the second flight telemetry data and is presented in Figure A-3. The data of this figure show a higher pitching frequency than the design prediction and later resonance time. This is important because the magnification factor increases with time up to burnout (Figure 24) and was higher for the second flight than either the first flight or predicted value. Now, depending upon the misalignments present, a certain trim angle will exist, which, when magnified enough can become quite large; large enough, it is conjectured, to diminish the roll efficiency of the fins upon which the vehicle is dependent to pass through resonance. It is believed that this is what occurred in the second flight and must be avoided to insure proper performance.

Consequently, for the next Archer flight the delayed ignition of the sustainer will be corrected and the fin-cant angle will be increased to 20 minutes. Calculations indicate that Archer should then pass through resonance at about 25 seconds of elapsed flight time and with a pitch frequency of approximately 3.75 cycles per second. This is still well on the descending side of the pitching frequency curve, affording a point crossover, and it is expected that the decrease realized in magnification factor will be sufficient to keep the vehicle trim angle and consequently roll rate within tolerable limits. Also beneficial will be the increased roll rate in minimizing the effects of any inherent misalignments in the system.

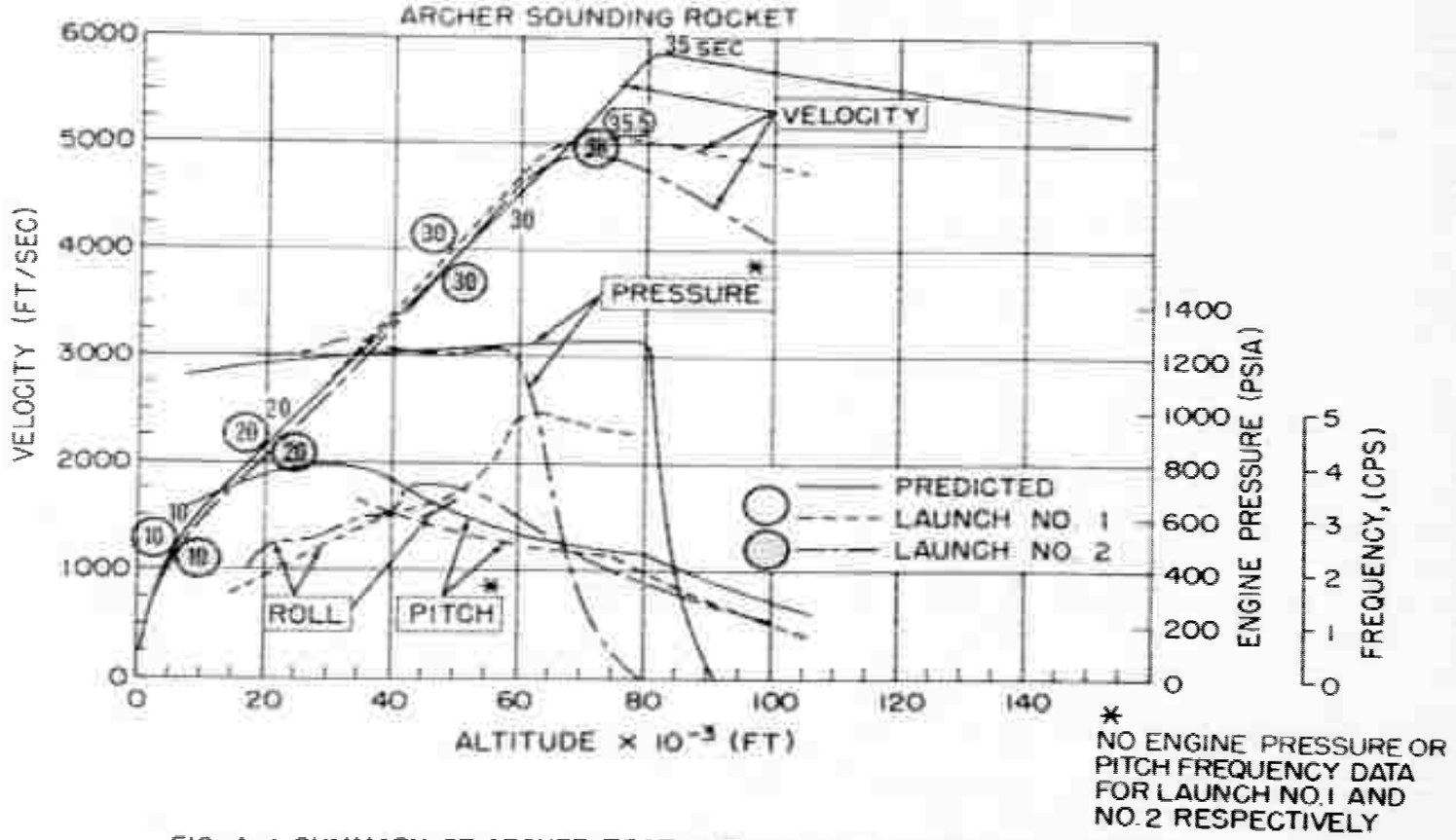

NOLTR 63-144

FIG. A-1 SUMMARY OF ARCHER TEST DATA AS A FUNCTION OF ALTITUDE

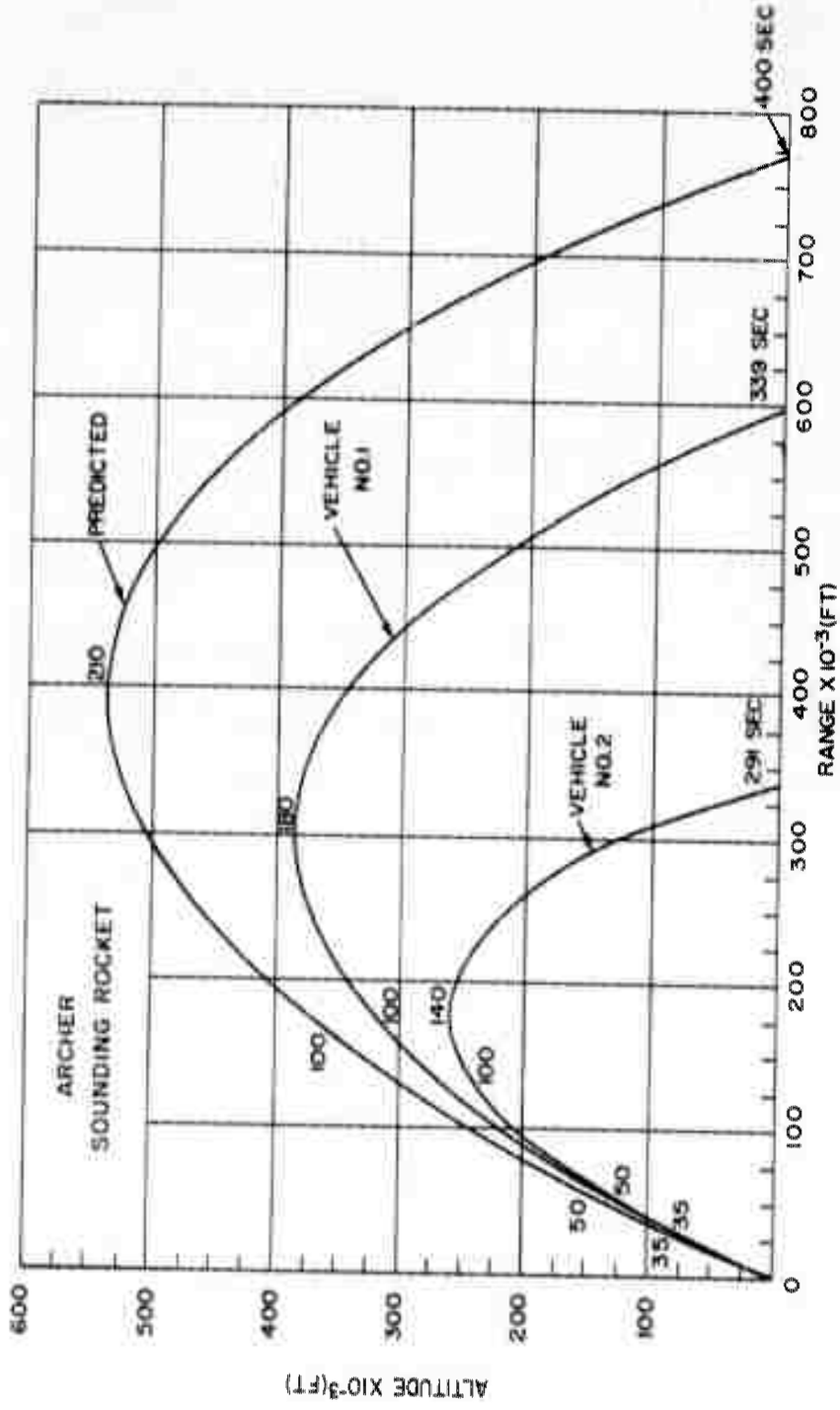

FIG. A-2 ALTITUDES ACHIEVED BY TEST VEHICLES NUMBER 182 AS A FUNTION OF RANGE

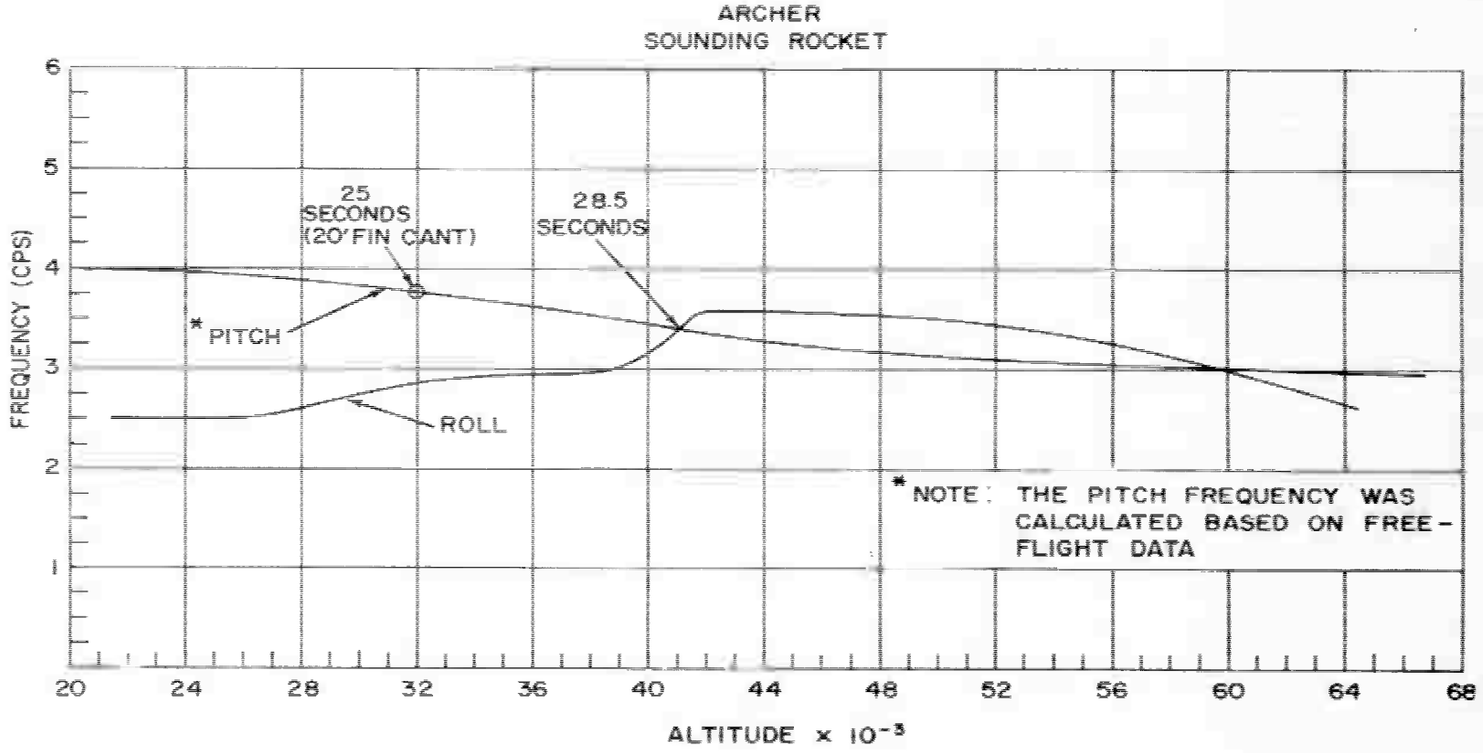

NOLTR 63-144

FIG. A-3 FLIGHT NUMBER 2-PITCH AND ROLL FREQUENCIES AS A FUNCTION OF ALTITUDE

AERODYNAMICS DEPARTMENT
EXTERNAL DISTRIBUTION LIST (A1)

	No. of Copies
Chief, Bureau of Naval Weapons Department of the Navy Washington 25, D. C.	
Attn: DLI-30	1
Attn: R-14	1
Attn: RRRE-4	1
Attn: RMGA-811	1
Attn: RMMO-42	1
Attn: RT	1
Attn: A. O. Conley, Jr. RTOS-41	1
Office of Naval Research Room 2709, T-3 Washington 25, D. C.	
Attn: Head, Mechanics Branch	1
Director, David Taylor Model Basin Aerodynamics Laboratory Washington 7, D. C.	
Attn: Library	1
Commander, U. S. Naval Ordnance Test Station China Lake, California	
Attn: Technical Library	1
Attn: Code 503	1
Attn: Code 406	1
Director, Naval Research Laboratory Washington 25, D. C.	
Attn: Code 2027	1
Attn: Dr. T. Chubb	1
Commanding Officer Office of Naval Research Branch Office Box 39, Navy 100 Fleet Post Office New York, New York	1
NASA High Speed Flight Station Box 273 Edwards Air Force Base, California	
Attn: W. C. Williams	1
NASA Ames Research Center Moffett Field, California	
Attn: Librarian	1
NASA Goddard Space Flight Center Beltsville, Maryland	
Attn: E.F. Sorgnit	1
Attn: Library	1

AERODYNAMICS DEPARTMENT
EXTERNAL DISTRIBUTION LIST (A1)

	No. of Copies
NASA Langley Research Center Langley Field, Virginia	
Attn: Librarian (Mrs. Elizabeth R. Gilman)	3
Attn: C. H. McLellan	1
Attn: J.J. Stack	1
Attn: Adolf Busemann	1
Attn: Comp. Res. Div.	1
Attn: Theoretical Aerodynamics Division	1
NASA Lewis Research Center 21000 Brookpark Road Cleveland 11, Ohio	
Attn: Librarian	1
Attn: Chief, Propulsion Aerodynamics Div.	1
NASA 1520 H Street, N. W. Washington 25, D. C.	
Attn: Chief, Division of Research Information	1
Attn: Dr. H. H. Kurzweg, Asst. Director of Research	1
Attn: M. Tepper	1
Office of the Assistant Secretary of Defense (R&D) Room 3E1065, The Pentagon Washington 25, D. C.	
Attn: Technical Library	1
Research and Development Board Room 3D1041, The Pentagon Washington 25, D. C.	
Attn: Library	1
DDC Cameron Stn Alexandria, Virginia 22314	20
Commander, Pacific Missile Range Point Mugu, California	
Attn: Technical Library	1
Attn: Ensign Charles Nichols, Code N-2221	1
Commanding General Aberdeen Proving Ground, Maryland	
Attn: Technical Information Branch	1
Attn: Ballistic Research Laboratory	1

AERODYNAMICS DEPARTMENT
EXTERNAL DISTRIBUTION LIST (A1)

	No. of Copies
Commander, Naval Weapons Laboratory Dahlgren, Virginia Attn: Library	1
Director, Special Projects Department of the Navy Washington 25, D. C. Attn: SP-2722	1
Director of Intelligence Headquarters, USAF Washington 25, D. C. Attn: AFOIN-3B	1
Headquarters - Aero. Systems Division Wright-Patterson Air Force Base Dayton, Ohio Attn: WWAD Attn: RRLA-Library	2 1
Commander Air Force Ballistic Missile Division HQ Air Research & Development Command P. O. Box 262 Inglewood, California Attn: WDTLAR	1
Chief, Defense Atomic Support Agency Washington 25, D. C. Attn: Document Library	1
Headquarters, Arnold Engineering Development Center Air Research and Development Center Arnold Air Force Station, Tennessee Attn: Technical Library Attn: AEOR Attn: AEOIM	1 1 1
Commanding Officer, DOFL Washington 25, D. C. Attn: Library, Room 211, Bldg. 92	1
Commanding General U. S. Army Missile Command Redstone Arsenal, Alabama Attn: AMSMI-RR(Mr. N. Shapiro) Attn: AMSMI-RB(Redstone Scientific Information Center)	1 1

AERODYNAMICS DEPARTMENT
EXTERNAL DISTRIBUTION LIST (A1)

	No. of Copies
NASA George C. Marshall Space Flight Center Huntsville, Alabama	
Attn: Dr. E. Geissler	1
Attn: Mr. T. Reed	1
Attn: Mr. H. Paul	1
Attn: Mr. W. Dahm	1
Attn: Mr. D. Burrows	1
Attn: Mr. J. Kingsbury	1
Attn: ORDAB-DA	1
Commander U.S. Air Force Cambridge Research Center Bedford, Mass.	
Attn: R. Palmquist	1
Attn: Library	1
APL/JHU (C-NOw 7386) 8621 Georgia Avenue Silver Spring, Maryland	
Attn: Technical Reports Group	2
Attn: Mr. D. Fox	1
Attn: Dr. F. Hill	1
Via: INSORD	
Air Force Systems Command Scientific and Technical Liaison Office Room 2305, Munitions Building Department of the Navy Washington 25, D.C.	
Attn: E. G. Haas	1
Mr. Foster F. Burgess Headquarters Air Proving Ground Center Code: PGWRR Eglin Air Force Base, Florida	1
Mr. R. G. Vande Vrede Atlantic Research Corporation Shirley Highway and Edsall Road Alexandria, Virginia	1
Commanding General U.S. Army Signal Missile Support Agency White Sands Proving Ground, N.M.	
Attn: W. Webb	1

AERODYNAMICS DEPARTMENT
EXTERNAL DISTRIBUTION LIST (A2)

No. of Copies

University of Minnesota
Minneapolis 14, Minnesota
Attn: Dr. E. R. G. Eckert
Attn: Heat Transfer Laboratory
Attn: Technical Library

Rensselaer Polytechnic Institute
Troy, New York
Attn: Dept. of Aeronautical Engineering

Dr. James P. Hartnett
Department of Mechanical Engineering
University of Delaware
Newark, Delaware

Princeton University
James Forrestal Research Center
Gas Dynamics Laboratory
Princeton, New Jersey
Attn: Prof. S. Bogdonoff
Attn: Dept. of Aeronautical Engineering Library

Defense Research Laboratory
The University of Texas
P. O. Box 8029
Austin 12, Texas
Attn: Assistant Director

Ohio State University
Columbus 10, Ohio
Attn: Security Officer
Attn: Aerodynamics Laboratory
Attn: Dr. J. Lee
Attn: Chairman, Dept. of Aero. Engineering

California Institute of Technology
Pasadena, California
Attn: Guggenheim Aero. Laboratory,
Aeronautics Library
Attn: Jet Propulsion Laboratory
Attn: Dr. H. Liepmann
Attn: Dr. L. Lees
Attn: Dr. D. Coles
Attn: Dr. A. Roshko
Attn: Dr. J. Laufer

Case Institute of Technology
Cleveland 6, Ohio
Attn: G. Kuerti

AERODYNAMICS DEPARTMENT
EXTERNAL DISTRIBUTION LIST (A2)

No. of Copies

North American Aviation, Inc.
Aerophysics Laboratory
Downey, California
Attn: Dr. E. R. Van Driest
Attn: Missile Division (Library)

Department of Mechanical Engineering
Yale University
400 Temple Street
New Haven 10, Connecticut
Attn: Dr. P. P. Wegener

MIT Lincoln Laboratory
Lexington, Massachusetts

RAND Corporation
1700 Main Street
Santa Monica, California
Attn: Library, USAF Project RAND
Attn: Technical Communications

Mr. J. Lukasiewicz
Chief, Gas Dynamics Facility
ARO, Incorporated
Tullahoma, Tennessee

Massachusetts Institute of Technology
Cambridge 39, Massachusetts
Attn: Prof. J. Kaye
Attn: Prof. M. Finston
Attn: Mr. J. Baron
Attn: Prof. A. F. Shapiro
Attn: Naval Supersonic Laboratory
Attn: Aero. Engineering Library
Attn: Prof. Ronald F. Probstein
Attn: Prof. C. C. Lin

Polytechnic Institute of Brooklyn
527 Atlantic Avenue
Freeport, New York
Attn: Dr. A. Ferri
Attn: Dr. M. Bloom
Attn: Dr. P. Libby
Attn: Aerodynamics Laboratory

Brown University
Division of Engineering
Providence, Rhode Island
Attn: Librarian

AERODYNAMICS DEPARTMENT
EXTERNAL DISTRIBUTION LIST (A2)

	No. of Copies
Air Ballistics Laboratory Army Ballistic Missile Agency Huntsville, Alabama	
Applied Mechanics Reviews Southwest Research Institute 3500 Culebra Road San Antonio 6, Texas	
BuWeps Representative Aerojet-General Corporation 6352 N. Irwindale Avenue Azusa, California	
The Boeing Company Seattle, Washington Attn: J. H. Russell, Aero-Space Division Attn: Research Library	
United Aircraft Corporation 400 Main Street East Hartford 8, Connecticut Attn: Chief Librarian Attn: Mr. W. Kuhrt, Research Dept. Attn: Mr. J. G. Lee	2
Hughes Aircraft Company Florence Avenue at Teale Streets Culver City, California Attn: Mr. D. J. Johnson R&D Technical Library	
McDonnell Aircraft Corporation P. O. Box 516 St. Louis 3, Missouri	
Lockheed Missiles and Space Company P. O. Box 504 Sunnyvale, California Attn: Dr. I. H. Wilson Attn: Mr. M. Tucker Attn: Dr. R. Smelt	
Martin Marietta Corp. Baltimore 3, Maryland Attn: Library Attn: Chief Aerodynamicist Attn: Dr. W. Morkovin Aerophysics Division	3

AERODYNAMICS DEPARTMENT
EXTERNAL DISTRIBUTION LIST (A2)

	No. of Copies
CONVAIR A Division of General Dynamics Corporation Fort Worth, Texas Attn: Library Attn: Theoretical Aerodynamics Group	
Purdue University School of Aeronautical & Engineering Sciences LaFayette, Indiana Attn: R. L. Taggart, Library	
University of Maryland College Park, Maryland Attn: Director Attn: Dr. J. Burgers Attn: Librarian, Engr. & Physical Sciences Attn: Librarian, Institute for Fluid Dynamics and Applied Mathematics Attn: Prof. S. I. Pai	2
University of Michigan Ann Arbor, Michigan Attn: Dr. A. Kuethe Attn: Dr. A. Laporte Attn: Department of Aeronautical Engineering	
Stanford University Palo Alto, California Attn: Applied Mathematics & Statistics Lab. Attn: Prof. D. Bershader, Dept. of Aero. Engr.	
Cornell University Graduate School of Aeronautical Engineering Ithaca, New York Attn: Prof. W. R. Sears	
The Johns Hopkins University Charles and 34th Streets Baltimore, Maryland Attn: Dr. F. H. Clauser	
University of California Berkeley 4, California Attn: G. Maslach Attn: Dr. S. A. Schaaf Attn: Dr. Holt Attn: Institute of Engineering Research	

AERODYNAMICS DEPARTMENT
EXTERNAL DISTRIBUTION LIST (A2)

No. of Copies

Cornell Aeronautical Laboratory, Inc.
4455 Genesee Street
Buffalo 21, New York
Attn: Librarian
Attn: Dr. Franklin Moore
Attn: Dr. J. G. Hall
Attn: Mr. A. Hertzberg

University of Minnesota
Rosemount Research Laboratories
Rosemount, Minnesota
Attn: Technical Library

Director, Air University Library
Maxwell Air Force Base, Alabama

Douglas Aircraft Company, Inc.
Santa Monica Division
3000 Ocean Park Boulevard
Santa Monica, California
Attn: Chief Missiles Engineer
Attn: Aerodynamics Section

CONVAIR
A Division of General Dynamics Corporation
Daingerfield, Texas

CONVAIR
Scientific Research Laboratory
5001 Kearney Villa Road
San Diego, California
Attn: Asst. to the Director of Scientific Research
Attn: Dr. B. M. Leadon
Attn: Library

Republic Aviation Corporation
Farmingdale, New York
Attn: Technical Library

General Applied Science Laboratories, Inc.
Merrick and Stewart Avenues
Westbury, L. I., New York
Attn: Mr. Walter Daskin
Attn: Mr. R. W. Byrne

AERODYNAMICS DEPARTMENT
EXTERNAL DISTRIBUTION LIST (A2)

	No. of Copies
Arnold Research Organization, Inc. Tullahoma, Tennessee Attn: Technical Library Attn: Chief, Propulsion Wind Tunnel Attn: Dr. J. L. Potter	
General Electric Company Missile Space Division 3198 Chestnut Street Philadelphia, Pennsylvania Attn: Larry Chasen, Mgr. Library Attn: Mr. R. Kirby Attn: Dr. J. Farber Attn: Dr. G. Sutton Attn: Dr. J. D. Stewart Attn: Dr. S. M. Scala Attn: Dr. H. Lew Attn: Mr. J. Persh	2
Eastman Kodak Company Navy Ordnance Division 50 West Main Street Rochester 14, New York Attn: W. B. Forman	2
Library AVCO-Everett Research Laboratory 2385 Revere Beach Parkway Everett 49, Massachusetts	3
Chance-Vought Corp. Post Office Box 5907 Dallas, Texas Library 1-6310/3L-2884	
National Science Foundation 1951 Constitution Avenue, N. W. Washington 25, D. C. Attn: Engineering Sciences Division	
New York University University Heights New York 53, New York Attn: Department of Aeronautical Engineering	

AERODYNAMICS DEPARTMENT
EXTERNAL DISTRIBUTION LIST (A2)

No. of Copies

New York University
25 Waverly Place
New York 3, New York
Attn: Library, Institute of Math. Sciences

NORAIR
A Division of Northrop Corp.
Hawthorne, California
Attn: Library

Northrop Aircraft, Inc.
Hawthorne, California
Attn: Library

Gas Dynamics Laboratory
Technological Institute
Northwestern University
Evanston, Illinois
Attn: Library

Pennsylvania State University
University Park, Pennsylvania
Attn: Library, Dept. of Aero. Engineering

The Ramo-Wooldridge Corporation
8820 Bellanca Avenue
Los Angeles 45, California

Gifts and Exchanges
Fondren Library
Rice Institute
P. O. Box 1892
Houston 1, Texas

University of Southern California
Engineering Center
Los Angeles 7, California
Attn: Librarian
Attn: Dr. R. Chaun

The Editor
Battelle Technical Review
Battelle Memorial Institute
505 King Avenue
Columbus 1, Ohio

Douglas Aircraft Company, Inc.
El Segundo Division
El Segundo, California

AERODYNAMICS DEPARTMENT
EXTERNAL DISTRIBUTION LIST (A2)

No. of Copies

FluiDyne Engineering Corp.
5740 Wayzata Blvd.
Golden Valley
Minneapolis 16, Minnesota

Grumman Aircraft Engineering Corp.
Bethpage, L. I., New York

Lockheed Missile and Space Company
P. O. Box 551
Burbank, California
Attn: Library

Marquardt Aircraft Corporation
7801 Havenhurst
Van Nuys, California

The Martin Company
Denver, Colorado
Attn: Library

The Martin Company
Orlando Division
Orlando, Florida
Attn: J. Mayer

Mississippi State College
Engineering and Industrial Research Station
Aerophysics Department
P. O. Box 248
State College, Mississippi

Lockheed Missile and Space Company
3251 Hanover Street
Palo Alto, California
Attn: Library

General Electric Company
Research Laboratory
Schenectady, New York
Attn: Dr. H. T. Nagamatsu
Attn: Library

Fluid Dynamics Laboratory
Mechanical Engineering Department
Stevens Institute of Technology
Hoboken, New Jersey
Attn: Dr. R. H. Page, Director

AERODYNAMICS DEPARTMENT
EXTERNAL DISTRIBUTION LIST (A2)

No. of Copies

Department of Mechanical Engineering
University of Arizona
Tucson, Arizona
Attn: Dr. E. K. Parks

Vitro Laboratories
200 Pleasant Valley Way
West Orange, New Jersey

Department of Aeronautical Engineering
University of Washington
Seattle 5, Washington
Attn: Prof. R. E. Street
Attn: Library

Aeronautical Engineering Review
2 East 64th Street
New York 21, New York

Institute of Aeronautics and Astronautics
500 Fifth Avenue
New York 36, New York
Attn: Managing Editor
Attn: Library

Department of Aeronautics
United States Air Force Academy
Colorado

MHD Research, Inc.
Newport Beach, California
Attn: Dr. V. H. Blackman, Technical Director

University of Alabama
College of Engineering
University, Alabama
Attn: Prof. C. H. Bryan, Head
Dept. of Aeronautical Engineering

ARDE Associates
100 W. Century Road
Paramus, New Jersey
Attn: Mr. Edward Cooperman

Aeronautical Research Associates of Princeton
50 Washington Road
Princeton, New Jersey
Attn: Dr. C. DuP. Donaldson, President

AERODYNAMICS DEPARTMENT
EXTERNAL DISTRIBUTION LIST (A2)

No. of Copies

Daniel Guggenheim School of Aeronautics
Georgia Institute of Technology
Atlanta, Georgia
Attn: Prof. A. L. Ducoffe

University of Cincinnati
Cincinnati, Ohio
Attn: Prof. R. P. Harrington, Head
Dept. of Aeronautical Engineering
Attn: Prof. Ting Yi Li, Aerospace Engineering Dept.

Virginia Polytechnic Institute
Dept. of Aerospace Engineering
Blacksburg, Virginia
Attn: Dr. R. T. Keefe
Attn: Dr. J. B. Eades, Jr.
Attn: Library

IBM Federal System Division
7220 Wisconsin Avenue
Bethesda, Maryland
Attn: Dr. I. Korobkin

Superintendent
U. S. Naval Postgraduate School
Monterey, California
Attn: Technical Reports Section Library

National Bureau of Standards
Washington 25, D. C.
Attn: Chief, Fluid Mechanics Section

North Carolina State College
Raleigh, North Carolina
Attn: Division of Engineering Research
Technical Library

Defense Research Corporation
P. O. Box No. 3587
Santa Barbara, California
Attn: Dr. J. A. Laurmann

Aerojet-General Corporation
6352 North Irwindale Avenue
Box 296
Azusa, California

AERODYNAMICS DEPARTMENT
EXTERNAL DISTRIBUTION LIST (A2)

No. of Copies

Apollo DDCS
General Electric Company
A&E Building, Room 204
Daytona Beach, Florida
Attn: Dave Hovis

University of Minnesota
Institute of Technology
Minneapolis, Minnesota
Attn: Prof. J. D. Akerman

Guggenheim Laboratory
Standord University
Stanford, California
Attn: Prof. D. Bershader, Dept. of Aero. Engineering

Space Technology Laboratory
Los Angeles, California
Attn: Dr. D. Bitondo

University of Illinois
Dept. of Aeronautical and A tronautical Engineering
Urbana, Illinois
Attn: Prof. H. S. Stilwell

Armour Research Foundation
Illinois Institute of Technology
10 West 35th Street
Chicago 16, Illinois
Attn: Dr. L. N. Wilson

Institute of the Aeronautical Sciences
Pacific Aeronautical Library
7600 Beverly Boulevard
Los Angeles 36, California

University of California
Dept. of Mathematics
Los Angeles, California
Attn: Prof. A. Robinson

Louisiana State University
Dept. of Aeronautical Engineering
College of Engineering
Baton Rouge, Louisiana

AERODYNAMICS DEPARTMENT
EXTERNAL DISTRIBUTION LIST (A2)

No. of Copies

Mathematical Reviews
American Mathematical Society
80 Waterman Street
Providence 6, Rhode Island

Stanford University
Dept. of Aeronautical Engineering
Stanford, California
Attn: Library

University of California
Aeronautical Sciences Laboratory
Richmond Field Station
1301 South 46th Street
Richmond, California

University of Denver
Dept. of Aeronautical Engineering
Denver 10, Colorado

University of Chicago
Laboratories for Applied Sciences
Museum of Science and Industry
Chicago 37, Illinois
Attn: Librarian

University of Colorado
Dept. of Aeronautical Engineering
Boulder, Colorado

University of Illinois
Aeronautical Dept.
Champaign, Illinois

University of Kentucky
Dept. of Aeronautical Engineering
College of Engineering
Lexington, Kentucky

University of Toledo
Dept. of Aeronautical Engineering
Research Foundation
Toledo, Ohio

University of Washington
Dept. of Aeronautical Engineering
Seattle, Washington
Attn: Librarian

AERODYNAMICS DEPARTMENT
EXTERNAL DISTRIBUTION LIST (A2)

No. of Copies

Aerospace Corporation
Advanced Propulsion and Fluid Mechanics Dept.
P. O. Box 95085
Los Angeles, California

Boeing Scientific Research Laboratory
P. O. Box 3981
Seattle 24, Washington
Attn: Dr. A. K. Srukanth
Attn: G. J. Appenheimer

Vidya, Inc.
2626 Hanover
Palo Alto, California
Attn: Mr. J. R. Stalder
Attn: Library

General Electric Co.
FPD Technical Information Center F-22
Cincinnati 15, Ohio

Northwestern University
Technological Institute
Evanston, Illinois
Attn: Dept. of Mechanical Engineering

Harvard University
Cambridge, Massachusetts
Attn: Prof. of Engineering Sciences and Applied Physics
Attn: Library

University of Wisconsin
P. O. Box 2127
Madison, Wisconsin
Attn: Prof. J. O. Hirschfelder

CATALOGING INFORMATION FOR LIBRARY USE

BIBLIOGRAPHIC INFORMATION

	DESCRIPTORS	CODES		DESCRIPTORS	CODES
SOURCE	NOL technical report	NOLTR	SECURITY CLASSIFICATION AND CODE COUNT	Unclassified ~ 25	UØ25
REPORT NUMBER	63-144	63Ø144	CIRCULATION LIMITATION		
REPORT DATE	14 June 1963	Ø663	CIRCULATION LIMITATION OR BIBLIOGRAPHIC		
			BIBLIOGRAPHIC (SUPPL., VOL., ETC.)		

SUBJECT ANALYSIS OF REPORT

DESCRIPTORS	CODES	DESCRIPTORS	CODES	DESCRIPTORS	CODES
Archer	ARCR	Payloads	PAYL	Missiles (design)	MISLD
Sounding	SOUN	Aerodynamic heating	AERY		
Rocket	MISL	Structure	STRC		
Development	DEVE	Weight	WEIO		
Single stage	SING	Performance	PERF		
High altitude	HIGA	Naval Research Laboratory	NRLA		
International Quiet Sun Year, 1964-1965	IQSY	Atlantic Research Corp.	ARCO		
Aerodynamics	AERD	Intermediate range	INTM		
Mechanics	MECA	Rocket motor	ROCK		
Configuration	COFI	NASA	NASA		
Stability	STBI	Propellants	FUEL		
Loads	LOAD	Specifications	SPEC		

Naval Ordnance Laboratory, White Oak, Md.
(NOL technical report 63-144)
THE DESIGN AND DEVELOPMENT OF THE ARCHER SOUNDING ROCKET (U), by H. J. Gauzza and others. 14 June 1963. 23p. illus., tables. (Aerodynamics research report 200) NOL task 625.

UNCLASSIFIED

The Naval Ordnance Laboratory has designed, developed and conducted free-flight tests on the Archer sounding rocket. Archer is an economical, single-stage sounding rocket capable of carrying a 25-pound payload to an altitude of 100 miles for IQSY studies. Archer's performance is predicted and comparisons are made with the results of the first two test firings.

1. Missiles - Archer
2. Missiles - Aerodynamics
3. International Quiet Sun Year, 1964-1965

I. Title
II. Gauzza, Harry J.
III. Series
IV. Project

Abstract card is unclassified.

Naval Ordnance Laboratory, White Oak, Md.
(NOL technical report 63-144)
THE DESIGN AND DEVELOPMENT OF THE ARCHER SOUNDING ROCKET (U), by H. J. Gauzza and others. 14 June 1963. 23p. illus., tables. (Aerodynamics research report 200) NOL task 625.

UNCLASSIFIED

The Naval Ordnance Laboratory has designed, developed and conducted free-flight tests on the Archer sounding rocket. Archer is an economical, single-stage sounding rocket capable of carrying a 25-pound payload to an altitude of 100 miles for IQSY studies. Archer's performance is predicted and comparisons are made with the results of the first two test firings.

1. Missiles - Archer
2. Missiles - Aerodynamics
3. International Quiet Sun Year, 1964-1965

I. Title
II. Gauzza, Harry J.
III. Series
IV. Project

Abstract card is unclassified.

Naval Ordnance Laboratory, White Oak, Md.
(NOL technical report 63-144)
THE DESIGN AND DEVELOPMENT OF THE ARCHER SOUNDING ROCKET (U), by H. J. Gauzza and others. 14 June 1963. 23p. illus., tables. (Aerodynamics research report 200) NOL task 625.

UNCLASSIFIED

The Naval Ordnance Laboratory has designed, developed and conducted free-flight tests on the Archer sounding rocket. Archer is an economical, single-stage sounding rocket capable of carrying a 25-pound payload to an altitude of 100 miles for IQSY studies. Archer's performance is predicted and comparisons are made with the results of the first two test firings.

1. Missiles - Archer
2. Missiles - Aerodynamics
3. International Quiet Sun Year, 1964-1965

I. Title
II. Gauzza, Harry J.
III. Series
IV. Project

Abstract card is unclassified.

Naval Ordnance Laboratory, White Oak, Md.
(NOL technical report 63-144)
THE DESIGN AND DEVELOPMENT OF THE ARCHER SOUNDING ROCKET (U), by H. J. Gauzza and others. 14 June 1963. 23p. illus., tables. (Aerodynamics research report 200) NOL task 625.

UNCLASSIFIED

The Naval Ordnance Laboratory has designed, developed and conducted free-flight tests on the Archer sounding rocket. Archer is an economical, single-stage sounding rocket capable of carrying a 25-pound payload to an altitude of 100 miles for IQSY studies. Archer's performance is predicted and comparisons are made with the results of the first two test firings.

1. Missiles - Archer
2. Missiles - Aerodynamics
3. International Quiet Sun Year, 1964-1965

I. Title
II. Gauzza, Harry J.
III. Series
IV. Project

Abstract card is unclassified.

Naval Ordnance Laboratory, White Oak, Md.
(NOL technical report 63-144)
THE DESIGN AND DEVELOPMENT OF THE ARCHER SOUNDING ROCKET (U), by H. J. Gauzza and others. 14 June 1963. 23p. illus., tables. (Aerodynamics research report 200) NOL task 625.

UNCLASSIFIED

The Naval Ordnance Laboratory has designed, developed and conducted free-flight tests on the Archer sounding rocket. Archer is an economical, single-stage sounding rocket capable of carrying a 25-pound payload to an altitude of 100 miles for IQSY studies. Archer's performance is predicted and comparisons are made with the results of the first two test firings.

1. Missiles - Archer
2. Missiles - Aerodynamics
3. International Quiet Sun Year, 1964-1965

I. Title
II. Gauzza, Harry J.
III. Series
IV. Project

Abstract card is unclassified.

Naval Ordnance Laboratory, White Oak, Md.
(NOL technical report 63-144)
THE DESIGN AND DEVELOPMENT OF THE ARCHER SOUNDING ROCKET (U), by H. J. Gauzza and others. 14 June 1963. 23p. illus., tables. (Aerodynamics research report 200) NOL task 625.

UNCLASSIFIED

The Naval Ordnance Laboratory has designed, developed and conducted free-flight tests on the Archer sounding rocket. Archer is an economical, single-stage sounding rocket capable of carrying a 25-pound payload to an altitude of 100 miles for IQSY studies. Archer's performance is predicted and comparisons are made with the results of the first two test firings.

1. Missiles - Archer
2. Missiles - Aerodynamics
3. International Quiet Sun Year, 1964-1965

I. Title
II. Gauzza, Harry J.
III. Series
IV. Project

Abstract card is unclassified.

Naval Ordnance Laboratory, White Oak, Md.
(NOL technical report 63-144)
THE DESIGN AND DEVELOPMENT OF THE ARCHER SOUNDING ROCKET (U), by H. J. Gauzza and others. 14 June 1963. 23p. illus., tables. (Aerodynamics research report 200) NOL task 625.

UNCLASSIFIED

The Naval Ordnance Laboratory has designed, developed and conducted free-flight tests on the Archer sounding rocket. Archer is an economical, single-stage sounding rocket capable of carrying a 25-pound payload to an altitude of 100 miles for IQSY studies. Archer's performance is predicted and comparisons are made with the results of the first two test firings.

1. Missiles - Archer
2. Missiles - Aerodynamics
3. International Quiet Sun Year, 1964-1965

I. Title
II. Gauzza, Harry J.
III. Series
IV. Project

Abstract card is unclassified.

Naval Ordnance Laboratory, White Oak, Md.
(NOL technical report 63-144)
THE DESIGN AND DEVELOPMENT OF THE ARCHER SOUNDING ROCKET (U), by H. J. Gauzza and others. 14 June 1963. 23p. illus., tables. (Aerodynamics research report 200) NOL task 625.

UNCLASSIFIED

The Naval Ordnance Laboratory has designed, developed and conducted free-flight tests on the Archer sounding rocket. Archer is an economical, single-stage sounding rocket capable of carrying a 25-pound payload to an altitude of 100 miles for IQSY studies. Archer's performance is predicted and comparisons are made with the results of the first two test firings.

1. Missiles - Archer
2. Missiles - Aerodynamics
3. International Quiet Sun Year, 1964-1965

I. Title
II. Gauzza, Harry J.
III. Series
IV. Project

Abstract card is unclassified.

UNCLASSIFIED